Mixed s-wave and d-wave superconductivity in high-T_c systems

Q. P. Li, B. E. C. Koltenbah, and Robert Joynt
Department of Physics and Applied Superconductivity Center, University of Wisconsin—Madison, 1150 University Avenue, Madison, Wisconsin 53706
(Received 30 December 1992)

We investigate the nature of the superconducting state of high-T_c materials from a microscopic theory and from a phenomenological analysis of experimental data. The simplest model for a microscopic electronic mechanism is the one-band Hubbard model, for which the parameters can be derived from experiment and cluster calculations. For these parameter values and moderate doping levels, we use the variational Monte Carlo method to show that a mixed s-d Cooper-pair state is favored. These results are compared to quantum Monte Carlo results on the Hubbard model. This mixed state is compared with experimental results on nuclear-magnetic-resonance relaxation times and Knight shifts, penetration depth, and tunneling measurements. The comparison with experiment indicates that a mixed-symmetry state is a strong candidate for the ground state of the system, comparing favorably to pure d-wave and pure s-wave states.

I. INTRODUCTION

A considerable body of work indicates that the phonon mechanism of superconductivity can produce only rather low critical temperatures (T_c's). The high T_c's of the layered cuprate materials therefore mark them out as possible candidates for an electronic mechanism.[1,2] Electronically generated pairing interactions can lead to unconventional (non-s-wave) Cooper-pair states because of nontrivial structure in momentum or spin space. The superfluidity of ^{3}He is a concrete example of this.[3,4] Heavy-fermion systems are most likely another, and in connection with the latter case, it has been discovered that antiferromagnetic fluctuations can give rise to d-wave pairing.[5] The cuprate materials appear in each case to be close to an antiferromagnetic instability, and in some cases strong antiferromagnetic correlations have been directly observed in the superconducting state. This situation calls for an investigation of unconventional pairing states, particularly the d-wave state, in high-T_c systems. We shall define this state and give a general review of symmetry classification and Ginzburg-Landau theory for all relevant states in Sec. II.

From a microscopic theoretical point of view, the first problem to be solved is a choice of model. We take the one-band Hubbard model as the simplest model which is at present consistent with all experimental facts. Zhang and Rice gave a construction of Wannier states which form a split-off, low-lying, partially filled band starting from an appropriate tight-binding Hamiltonian with strong on-site repulsion.[6] This results in the t-J model. Later numerical studies on clusters and comparison with spectroscopic measurements confirmed that their description is consistent with the known low-lying levels.[7,8] It has also become clear that the complex NMR results in the normal state are explicable in a one-band model.[9,10] The t-J model therefore gives a reasonable description of the system energetics on scales of J and t, i.e., 0.05–1 eV. This does not by any means guarantee that the t-J model is adequate for the description of superconductivity. In the phonon case it is a "small" residual interaction which counters the "large" Coulomb interaction and gives rise to superconductivity. Our philosophy in this paper, however, is that one should search carefully for superconductivity in a minimal model before going on to consider the addition of more bands, excitons, plasmons, phonons, and so on. An additional complication which is ignored in our two-dimensional (2D) model is the interlayer coupling.[11] If interlayer pairing is operative, then this is a mistake, but the fact that T_c appears to be more or less independent of uniaxial stress perpendicular to the planes in fully oxygenated $YBa_2Cu_3O_7$ suggests that the pairing mechanism should be sought in the plane.[12,13]

Our Hamiltonian is

$$\begin{aligned} H = & -t \sum_{\langle i,j\rangle,\sigma} (c^\dagger_{i,\sigma} c_{j,\sigma} + c^\dagger_{j,\sigma} c_{i,\sigma}) \\ & + J \sum_{\langle i,j\rangle} (\mathbf{S}_i \cdot \mathbf{S}_j - \tfrac{1}{4} n_i n_j) \\ & - \tfrac{1}{4} J \sum_{i,\tau\neq\tau',\sigma} (c^\dagger_{i+\tau,\sigma} c^\dagger_{i,-\sigma} c_{i,-\sigma} c_{i+\tau',\sigma} \\ & \qquad + c^\dagger_{i+\tau,-\sigma} c^\dagger_{i,\sigma} c_{i,-\sigma} c_{i+\tau',\sigma}). \end{aligned} \tag{1}$$

H is understood to act on a square lattice on which double occupancy is forbidden. We will generally concentrate on the case of $J/t = \frac{1}{4}$, which is roughly the ratio deduced from the spectroscopic experiments and cluster calculations. When this ratio is fixed, all energies may be quoted in units of t, which is about 0.5 eV.[8] The Hamiltonian (1) follows from the Hubbard model with $U/t \gg 1$. The final term in H is the three-site term. It is often ignored because of its complexity and because it is proportional to J times the hole density per site δ. We find that for $\delta \geq 0.1$ it becomes quantitatively important, and so it is always kept in what follows.

We use the variational Monte Carlo (VMC) method[14] to determine the ground state of H. We describe this in some detail below. This approach contrasts with other methods, among which we mention two because of the similarity of the input physics. The quantum Monte Carlo (QMC) method has been used extensively in studies of possible superconductivity in the Hubbard model.[15] The results of these studies have on the whole been taken as evidence against superconductivity in the model. We argue in Sec. III that rather large lattices and strong coupling must be used to establish superconductivity in this model and QMC has not yet reached these sizes and coupling strengths. The spin fluctuation (SF) method[16] is based on ideas similar to those put forward here and in earlier papers, namely, that spin fluctuations are responsible for unconventional pairing. The Hamiltonian used in the SF method is not microscopic as ours is; on the other hand the phenomenological input (the wave-vector- and frequency-dependent susceptibility) is taken from experiment and should therefore be reasonably accurate. The method also has the advantage that standard approaches may be used to compute experimentally measurable finite frequency and finite temperature quantities. The VMC method cannot do this at present. The Hamiltonian of the SF method needs a coupling constant approaching 1 eV to produce high T_c's. Whether such a Hamiltonian can be derived from the t-J model we use is an open question.[17] Our conclusions about d-wave superconductivity in Sec. III below are mostly in agreement with the SF method, but there are crucial differences at high doping levels. The SF method produces only d-wave pairing, but we find that mixed s- and d-wave pairing also has a region of stability. We also note that SF calculations have generally been restricted to computation of the highest T_c among the different representations on a square lattice. This approach cannot find ground-state mixing.

The phenomenological part of the paper focuses on mixed s-wave and d-wave states, since the pure s- and d-wave states have been considered extensively in recent work. The comparison of d-wave states to experiment has recently been reviewed.[18,19] Generally, it appears that the d-wave state does somewhat better than the s-wave state. We will argue in Sec. V that mixed s- and d-wave states can improve on d-wave states.

The rest of the paper is organized as follows. In Sec. II we discuss the symmetry and the Ginzburg-Landau theory in the tetragonal and the orthorhombic lattices. We present the results of our VMC study of the t-J model on 2D square lattices of various sizes using a trial wave function for the d-wave pairing state in Sec. III. We show that the d-wave state has lower energy than the "normal state" on a large enough lattice (> 100 sites). We devote Sec. IV to the VMC studies of other pairing states. We find that a mixed s- and d-wave state is preferred over both the pure d-wave and the pure s-wave pairing states. In Sec. V we calculate the density of states for various pairing states and compare the theory with experiments, especially the magnetic penetration depth measurement. We phenomenologically analyze the nuclear-magnetic-resonance (NMR) data in $YBa_2Cu_3O_7$ using various pairing states in Sec. VI, which lends further support for the mixed s- and d-wave state. We conclude the paper with some discussions in Sec. VII. Some of the work presented here has been published previously in short communications.[20–22]

II. SYMMETRY PROPERTIES

The high-T_c materials are generally orthorhombic. This is true of the Bi-based materials, which have a superlattice modulation which distorts the tetragonal structure. The orthorhombic distortion is usually small, with a difference between the a and b axes of about 2% in $YBa_2Cu_3O_7$,[13] for example. For this reason we treat the simpler case of tetragonal symmetry first, and then modify this for the actual orthorhombic case.

A. Tetragonal symmetry

The s-wave and d-wave states considered in this paper belong to the A_1 and B_1 representations of the tetragonal point group C_{4v}, corresponding to gap functions such as $\cos k_x a + \cos k_y a$ and $\cos k_x a - \cos k_y a$, respectively.[23] These representations are one dimensional, meaning that pure ordering in either state would be characterized by the growth of an order parameter which is a single complex number. Also note that s-wave and extended s-wave states are not distinguishable on symmetry grounds and therefore we defer discussion of this distinction to a later section. This B_1 d-wave state for high-T_c systems is quite different from the d-wave states proposed for heavy-fermion systems such as the E_1 state of hexagonal UPt_3. The E_1 representation is two dimensional and therefore has a pair of complex order parameters.

Mixed ordering in A_1 and B_1 in the tetragonal system would produce two order parameters. This is not forbidden in general; however, the two components would have different critical temperatures. The Ginzburg-Landau free-energy density in the absence of external field reads

$$f = \alpha_s(T - T_s)|\psi_s|^2 + \alpha_d(T - T_d)|\psi_d|^2 + \beta_s|\psi_s|^4 + \beta_d|\psi_d|^4 + \beta_{sd}|\psi_s|^2|\psi_d|^2 + \beta_p(\psi_s^2\psi_d^{*2} + \psi_s^{*2}\psi_d^2). \quad (2)$$

This expression shows a second-order transition at $T = \max(T_s, T_d)$ and may show a second second-order transition to a mixed phase if T_s and T_d are sufficiently close. There is no convincing experimental evidence for the occurrence of two transitions in the specific-heat measurements so far carried out in high-T_c systems (again in contrast to UPt_3). This apparently presents a problem for certain mean-field theories of superconductivity of the t-J model and for the mixed A_1-B_1 state we examine later. In these theories the s-wave and d-wave states are degenerate near half-filling and might be expected to be nearly degenerate at experimental doping levels. We shall argue below that considerations of the orthorhombic distortion of real systems removes this problem.

The free-energy density of a pure s-wave system in a field is, as usual,

$$f_s = \alpha_s(T - T_s)|\psi_s|^2 + \beta_s|\psi_s|^4 + K_s^{xy}(|p_x\psi_s|^2 + |p_y\psi_s|^2) + K_s^z|p_z\psi_s|^2, \quad (3)$$

where $p_x = -i\frac{\partial}{\partial x} - \frac{2eA_x}{\hbar c}$, etc. The free energy of the d-wave system is precisely isomorphic:

$$f_d = \alpha_d(T - T_d)|\psi_d|^2 + \beta_d|\psi_d|^4 + K_d^{xy}(|p_x\psi_d|^2 + |p_y\psi_d|^2) + K_d^z|p_z\psi_d|^2. \quad (4)$$

In fact all one-dimensional representations have exactly the same free energy. This is a general result not specific to C_{4v}. All elements of finite groups are of finite order; if the representation is one dimensional, all elements are therefore represented by a phase, the phase of a given element depending on the representation. Any term in the free energy of a superconductor must be invariant with respect to changes in phase because of gauge invariance to start with. Therefore the transformation properties of any term do not depend on the representation. To give a specific example relevant here, the term $K_s^{xy}(p_x\psi_s p_x^*\psi_s^* + p_y\psi_s p_y^*\psi_s^*)$ from Eq. (3) above transforms to $K_s^{xy}[(-p_y\psi_s)(-p_y^*\psi_s^*) + (p_x\psi_s)(p_x^*\psi_s^*)] = K_s^{xy}(|p_x\psi_s|^2 + |p_y\psi_s|^2)$ under a 90° rotation. The same term in Eq. (4) transforms as

$$K_d^{xy}(p_x\psi_d p_x^*\psi_d^* + p_y\psi_d p_y^*\psi_d^*)$$

$$\rightarrow K_d^{xy}[(-p_y)(-\psi_d)(-p_y^*)(-\psi_d^*) + p_x(-\psi_d^*)p_x^*(-\psi_d^*)] = K_d^{xy}(|p_x\psi_d|^2 + |p_y\psi_d|^2).$$

Terms invariant in A_1 are guaranteed to be invariant in B_1 and conversely. This theorem has an important consequence for d-wave theories of high-T_c systems: There is no way to distinguish s-wave and d-wave theories by experiments whose results depend only on the *form* of Ginzburg-Landau theory. If high-T_c materials are d wave, the whole phenomenology of flux lattices, pinning, creep, etc., may be taken over without modification except that the calculation of the parameters appearing in f from microscopic theory would be different in s- and d-wave cases.

If s-d mixing is allowed, there is an additional, rather strange-looking gradient term in the free-energy density: $f_{sd} = K_{sd}(p_x\psi_s p_x^*\psi_d^* - p_y\psi_s p_y^*\psi_d^* + \text{c.c.})$. Thus, a mixed phase can have modified H_{c_2} curves, as discussed in Ref. 22. The existence of gradient terms in mixed states from the general group-theoretical point of view is also discussed in this reference. What we term the "$s+id$" state in this paper is any state of the form

$$\Delta(\mathbf{k}) = \psi_s(\cos k_x + \cos k_y) + i\psi_d(\cos k_x - \cos k_y), \quad (5)$$

where the relative phase of ψ_s and ψ_d is $e^{i\pi/2}$. We assume lattice constant a=1 throughout this paper. For the case when $\psi_s = \psi_d$, we have

$$\Delta(\mathbf{k}) = \psi_s[(1+i)\cos k_x + (1-i)\cos k_y] \quad (6)$$

$$= (1+i)\psi_s(\cos k_x - i\cos k_y), \quad (7)$$

and $\Delta^*(\mathbf{k}) = (1-i)\psi_s^*(\cos k_x + i\cos k_y)$. This gap is the same as that found originally by Kotliar.[24] It is often called the $s+id$ state. We are thus using this term in a slightly extended sense.

B. Orthorhombic symmetry

We now turn to orthorhombic symmetry, with point group C_{2v}. C_{2v} is obtained from C_{4v} by deleting 90° rotations about the c axis and reflections in the $x = \pm y$ lines. These are precisely the operation under which the d-wave state transforms nontrivially, i.e., with change of sign. Under all the operations of C_{2v}, the d-wave (B_1 in C_{4v}) state is invariant, meaning that it transforms as A_1, the identity representation, or the *s-wave* representation. In orthorhombic symmetry, *s wave and d wave are the same* from the point of view of symmetry. Thus there is only one order parameter. There is only one critical temperature, in agreement with experiment. The Ginzburg-Landau free energy is

$$f = \alpha|\psi|^2 + \beta|\psi|^4 + \sum_i K_i|p_i\psi|^2, \quad (8)$$

where $i = x, y, z$ and $K_x \neq K_y \neq K_z$. This free energy governs thermodynamics near T_c. Any anisotropy in the state is crystalline anisotropy—not unconventional superconductivity. See Fig. 1 for an illustration of this point. Also note that the peculiar gradient term in the mixed s-d state in tetragonal symmetry goes over into,

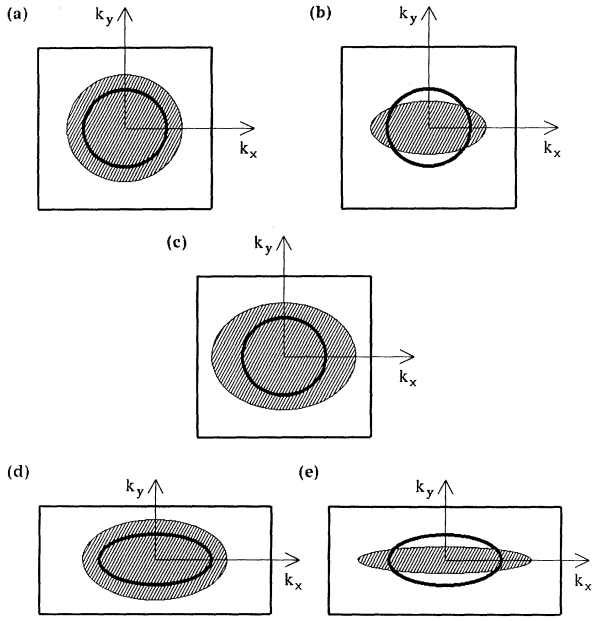

FIG. 1. Symmetry properties of s-wave and d-wave states in tetragonal and orthorhombic crystals. The thick line is the Fermi surface. The curve enclosing the shaded region represents the gap function. (a) s-wave state in tetragonal lattice; (b) d-wave state in tetragonal lattice; (c) $s+d$ state in tetragonal lattice; (d) s-wave state in orthorhombic lattice; (e) d-wave state in orthorhombic. (d) and (e) are identical from the point of view of symmetry.

in effect generates, the difference between the gradient terms in the x and y directions in orthorhombic symmetry.

Theories of d-wave symmetry for high-T_c systems become s-wave theories in the real orthorhombic systems. This does not change the fact that there may be nodes of the gap, etc. It does mean that d-wave gap functions such as $\Delta(\mathbf{k}) \sim \cos k_x - \cos k_y$ will inevitably mix with s-wave gaps such as $\Delta(\mathbf{k}) \sim$ const, for all $T \leq T_c$.

Since the orthorhombic distortion is small, it is also interesting to treat it as a perturbation of C_{4v}, by adding a small effective field to the C_{4v} free energy. Then we find

$$f = f_s + f_d + f_{sd} + r(\psi_s^* \psi_d + \psi_s \psi_d^*). \tag{9}$$

If this free energy is minimized, we find that at T_c a combination of ψ_s and ψ_d arises. The combination may be obtained by diagonalizing the quadratic form $\alpha_s(T - T_s)|\psi_s|^2 + \alpha_d(T - T_d)|\psi_d|^2 + r(\psi_s^* \psi_d + \psi_s \psi_d^*)$ and finding the smallest coefficient. T_c is determined by setting this coefficient equal to zero. The eigenfunction corresponding to the lowest coefficient gives the s-d mixing near T_c. The lower transition then turns into a crossover, with the specific-heat jump smoothed out. What this theory describes is the temperature dependence of crystalline gap anisotropy below T_c. This gap anisotropy may be very important for calculation of microscopic properties, as we shall see in the later sections.

This simple expression already makes an experimental prediction. r must be proportional to the deviation from orthorhombic symmetry. In the tetragonal system $r = 0$ and there are two sharp transitions. As r increases, the lower transition broadens and is pushed down, but the upper transition is pushed further up; i.e., T_c should increase as the system becomes more orthorhombic. This is in contradiction, superficially, to experimental results on $YBa_2Cu_3O_7$, where T_c increases as the length of the a and b axes are made closer by uniaxial stress.[12,13] However, even when they are equal, $YBa_2Cu_3O_7$ is not tetragonal because of the Cu-O chains, and T_c may well be affected by compressing the chain because of charge transfer to the planes. In doped La_2CuO_4, on the other hand, T_c does apparently decrease as (true) tetragonality is approached.[25]

III. VMC RESULTS FOR THE d-WAVE STATE

Recent QMC calculations of the two-dimensional one-band Hubbard model have shown no evidence of d-wave pairing at finite temperatures for square lattice systems of finite size. This lack of d-wave pairing has led the QMC investigators to conclude that the Hubbard model may not support superconductivity.[15] In this section we present results of VMC calculations conducted on two-dimensional square lattices of finite size. Assuming a d-wave state for the t-J model, we have calculated that, for certain hole densities and lattices above a certain size, the energy of the d-wave pairing state is less than the normal-state energy, thereby showing evidence of superconductivity in this model. In addition to presenting our VMC results, we offer comparisons to QMC in order to understand why it apparently does not find superconductivity.

In brief, the VMC method is a random-walk importance-sampling technique which estimates expectation values of operators in given variational wave functions.[26] Our variational wave function is

$$|\psi\rangle = P_N P_D \prod_{\mathbf{k}} (u_{\mathbf{k}} + v_{\mathbf{k}} c_{\mathbf{k}\uparrow}^\dagger c_{-\mathbf{k}\downarrow}^\dagger) \,|\, 0\rangle. \tag{10}$$

Here P_N is the projection onto the N-particle subspace and P_D is the Gutzwiller projection onto the subspace of no-doubly-occupied sites.[21] $u_{\mathbf{k}}$ and $v_{\mathbf{k}}$ are the usual BCS coefficients for a momentum-dependent gap function and

$$a(\mathbf{k}) \equiv \frac{v_{\mathbf{k}}}{u_{\mathbf{k}}} = \frac{\Delta_d(\mathbf{k})}{\xi_{\mathbf{k}} + \sqrt{\xi_{\mathbf{k}}^2 + \Delta_d(\mathbf{k})^2}}, \tag{11}$$

where $\xi_{\mathbf{k}} = -2t(\cos k_x + \cos k_y) - \mu$, μ is the Fermi energy, and

$$\Delta_d(\mathbf{k}) = \psi_d(\cos k_x - \cos k_y) \tag{12}$$

is the d-wave gap function, where ψ_d is a variational gap parameter. (It is to be stressed that ψ_d is a parameter in our wave function. It is *not* the gap which would be observed in a tunneling or photoemission experiment. This is seen particularly clearly by noting that the "gap" ψ_d may be finite even at half-filling, when the order parameter for superconductivity vanishes.) Assuming a certain gap parameter ψ_d, hole density per site δ, and lattice size N, the ground-state energy E_G for this particular set of parameters is found by using the VMC technique to compute the expectation value of the Hamiltonian given in Eq. (1). Comparison of this energy with the energy of the "normal state" ($\psi_d = 0$) shows whether the d-wave pairing reduces the energy for that particular hole density and lattice size.[14]

We have conducted a VMC study of small, finite-sized systems with lattice sizes of 16, 26, 36, 50, 64, 82, and 100 sites with periodic boundary conditions. The "tilted" lattices of 26, 50, and 82 sites are also used in our calculations, in which case the period vectors are not along the (0,1) and (1,0) directions. The variational gap parameter ψ_d was varied from 0.0 to 1.0t. The hole density δ was set to 0.125, 0.250, and 0.375. These values of δ are the only choices available for the 16-site lattice if the constraints of no-doubly-occupied sites and no net magnetization are to be met. The corresponding δ values used for some of the larger lattice sizes were only approximately the same as these three values since they had to be altered slightly to meet these two constraints. In this section we concentrate on d-wave order parameters because we want to compare with QMC calculations which calculate the d-wave pairing susceptibility.

In Fig. 2(a) we show the VMC results for the d-wave state energy as a function of ψ_d for systems of 16, 26, and 36 sites and a hole density of 0.125. It is clear that the lowest energies calculated for the 16- and 26-site lattices are those corresponding to the normal ($\psi_d = 0$) state. The 36-site results also show no conclusive evidence of d-wave pairing since the minimum of the energy at finite ψ_d is well within statistical uncertainty. Figure 2(b) shows

the results of the same calculations performed on the 50-, 64-, 82-, and 100-site lattices. The upward concavity of the 26- and 50-site energy plots and downward concavity of the 16-, 36-, and 64-site curves indicate that these small-sized systems are greatly affected by finite-size effects. Here again there is clearly no finite-gap minimum in the 50-site results and there is no conclusive evidence of d-wave pairing outside of statistical noise in the 64- and 82-site systems. However, the 82-site results do not show that same downward concavity seen in the plots of the energies of the other tilted lattices, and this may indicate that the 82-site lattice is large enough or nearly large enough to suppress the finite-size effect. Indeed it is only the 100-site lattice which conclusively shows a minimum ground-state energy corresponding to a variational gap parameter value of approximately $0.2t$. The same VMC calculations were performed on an even larger lattice of 226 sites, and the results are shown in Fig. 2(c). Again it is clear that a d-wave state with $\psi_d \approx 0.2t$ is preferred over the $\psi_d = 0$ normal state.

Figures 3(a) and 3(b) show further energy calculations for $\delta \approx 0.250$ on lattices of 16–64 sites. Figure 3(c) shows the same calculations for $\delta \approx 0.375$. Here again there is no evidence of d-wave pairing outside of statistical uncer-

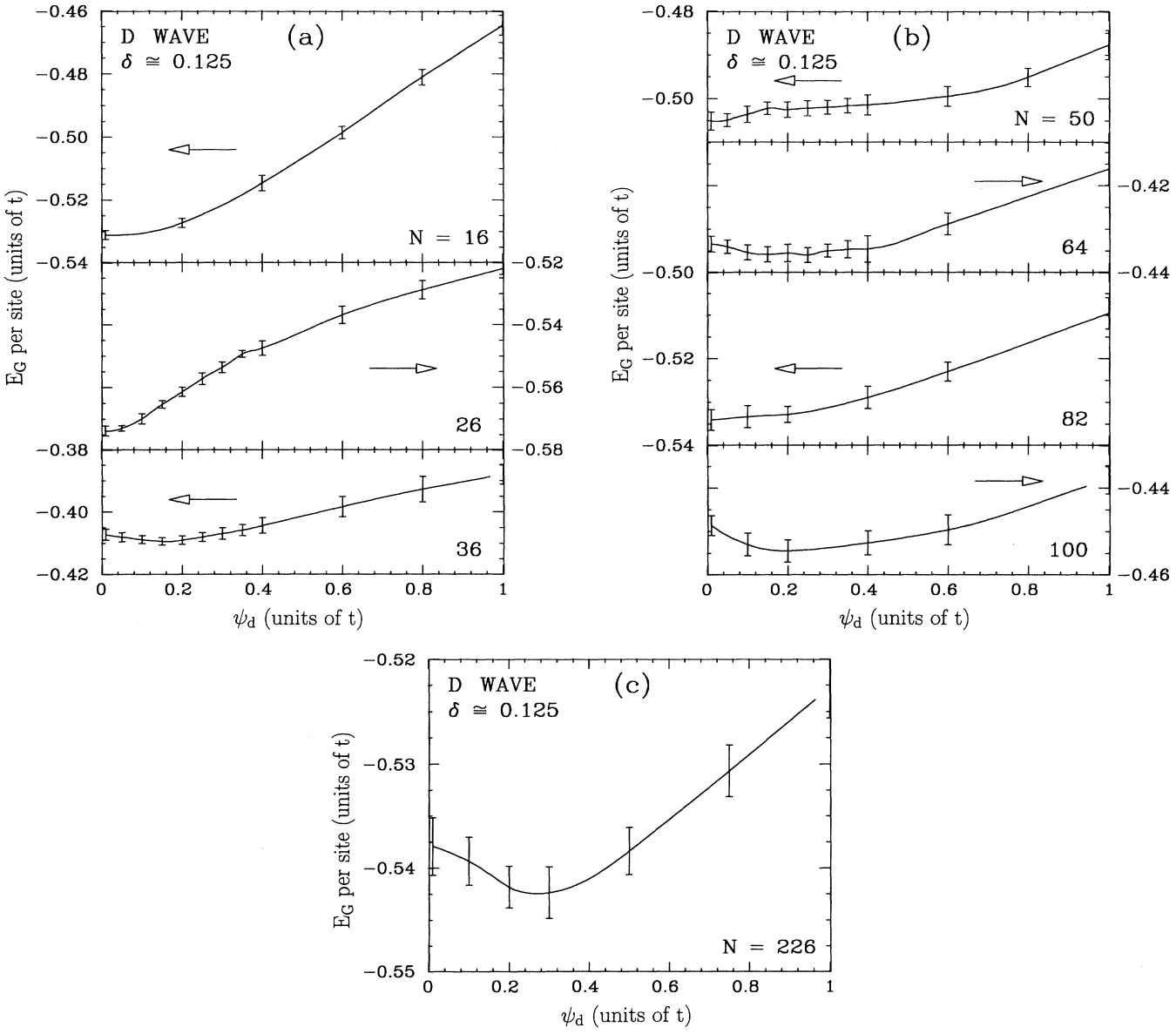

FIG. 2. Shows the calculated energy expectation value vs variational gap parameter ψ_d for $\delta \approx 0.125$ on lattice sizes of (a) 16, 26, and 36 sites, (b) 50, 64, 82, and 100 sites, and (c) 226 sites. All ground-state energies in Secs. III and IV are given in units of t per hole; all gap parameters are in t. Accepted Monte Carlo steps per site range from approximately 50×10^3 for the 16-site to 900 for the 226-site calculations.

tainty for these small lattice sizes examined. Again, this supports our conclusion that finite-size effects are dominant in these systems. Earlier VMC work has shown for larger lattice sizes that d-wave pairing is still preferred over the normal state for even larger hole densities,[21] but clearly that is not the case here for lattice sizes of 64 sites and less.

These results of the d-wave energy calculations on lat-

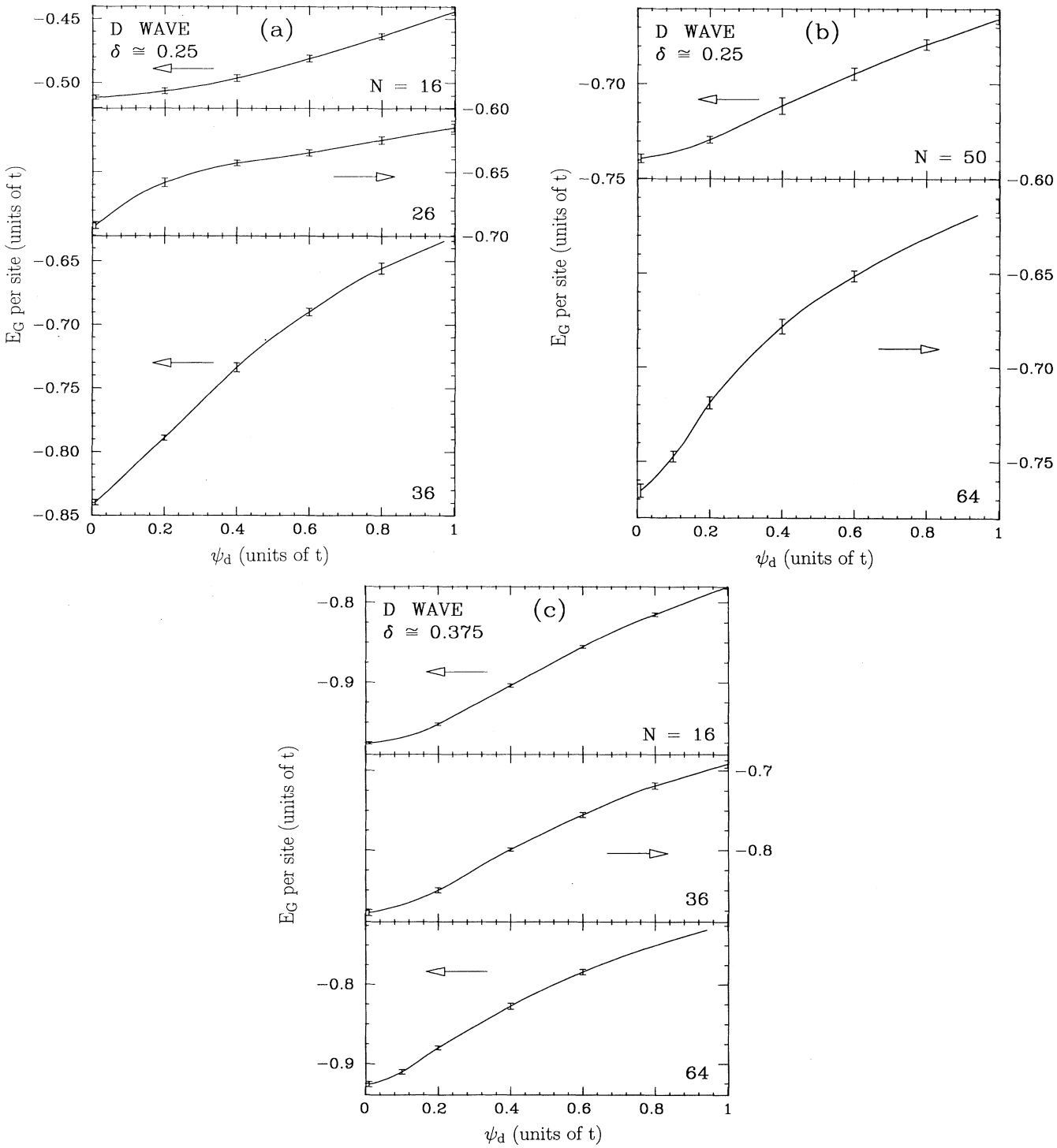

FIG. 3. Shows the calculated energy expectation value vs variational gap parameter ψ_d (a) for $\delta \approx 0.250$ and lattice sizes of 16, 26, and 36 sites, (b) for $\delta \approx 0.250$ and lattice sizes of 50 and 64 sites, and (c) for $\delta \approx 0.375$ and lattice sizes of 16, 36, and 64 sites.

tices of various sizes indicate that a minimum system size of about 100 sites is necessary for d-wave pairing to overcome finite-size effects. The results further indicate that the t-J model can support d-wave superconductivity at that minimum size of 100 sites for a hole density of around 0.125. The question then arises, do these VMC results of the existence of superconductivity for certain parameter values contradict the QMC conclusions of no d-wave pairing in Hubbard model? We believe our results are not necessarily at odds with the QMC work cited above for three reasons. First, the QMC calculations were done on the one-band positive-U Hubbard model in the intermediate-coupling regime, typically at $U/t = 4$, whereas our VMC investigation was on the t-J model, a large-U limit of the Hubbard model. Our value of $J/t = \frac{1}{4}$ corresponds to $U/t = 16$, but as stressed in Sec. I, this strong-coupling value is suggested by experiment. A second reason for these differing results between our work and QMC investigations could simply be due to the fact that the QMC calculations cited above were performed at finite temperature T, whereas our VMC work is restricted to calculating ground-state energies at $T = 0$. The QMC calculations become more and more computationally restricted as the temperature is reduced, and results are available only for $k_BT/t > 0.1$, where parameter values are typically $U = 4t$, $\delta = 0.125$, 0.5, and $N = 16$, 64.[15,27] k_BT_c/t is certainly less than 0.05 in high-T_c systems, and is probably closer to 0.02.

A third possible reason for the differing conclusions of VMC and QMC investigations is the size of the systems studied. We have shown that at least 100 sites were needed to conclusively show a preference of d-wave pairing over the normal state in these systems. With our VMC technique we find that lattice sizes greater than 100 sites are necessary—only above this do ground state energies begin to level off. QMC investigations of superconductivity are usually done on 16-site lattices. We have not been able to find work on systems larger then 64 sites. We believe there is an inherent problem in studying superconductivity, particularly d-wave superconductivity, in these smaller systems. Figure 4 shows the 16 allowed k vectors for the 16-site system. Shown above each k vector is the value $\Delta_d(\mathbf{k})/\psi_d$. Note that of the 16 values shown for each distinct k vector, 6 (or 37.5%) have the value 0, corresponding to node points in the d-wave gap function. If one concentrates on the Fermi surface, the situation is even worse, 4 out of 6 (i.e., 66.7%) of the states on the Fermi surface have $\Delta(\mathbf{k}) = 0$. For the 64-site system, only 14 (or 21.9%) of the 64 values of the d-wave gap function are 0, and this fraction of d-wave node points continues to decrease as the size of the system increases, where the increasing number of allowed k vectors better models a continuum of k states as $N \to \infty$. In other words, with so few k vectors and electronic states available in the smaller-sized systems, the d-wave gap function vanishes over a large fraction of the allowed points in k space. In addition to this problem, the differences in kinetic energy between neighboring k states is so large that a gap would have to overcome quite a step in kinetic energy to form; i.e., shell effects in momentum space are very important.

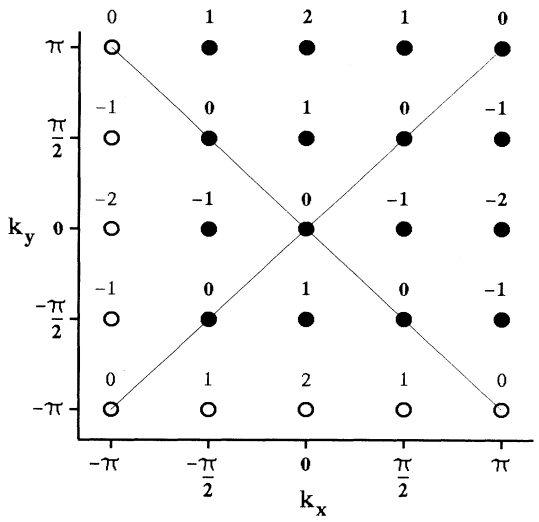

FIG. 4. Shows the 16 allowed k vectors in k space for the 16-site lattice. The black spots indicate the allowed k vectors, and the white spots, each corresponding 2π periodically to one of the 16 allowed k vectors, are only shown as a guide for the eye and to balance the figure. Shown above each k vector is $\Delta_d(\mathbf{k})/\psi_d$ in units of t. The node lines are shown where the d-wave gap function, Eq. (12), is zero.

In addition, there is an important difference between s-wave and d-wave superconductivity which arises in finite-size systems. It is crucial to have a large system if one wishes to locate the d-wave instability. The linearized gap equation is

$$\Delta(\mathbf{k},\omega_n) = -T\sum_{m,\mathbf{k}'} \frac{V_{\mathbf{k},\mathbf{k}'}(\omega_n-\omega_m)\Delta(\mathbf{k}',\omega_m)}{\omega_m^2+(\epsilon_{\mathbf{k}'}-\mu)^2}, \quad (13)$$

in a finite-size system. Here $V_{\mathbf{k},\mathbf{k}'}$ is an effective interaction, and the ω_n are Matsubara frequencies. A d-wave solution arises from the part of summation where $\mathbf{k}$ and $\mathbf{k}'$ are at or near the Fermi surface, and $V_{\mathbf{k},\mathbf{k}'}$ is large. This will be unlikely to occur when there are only 6 $\mathbf{k}$ points on the Fermi surface and at 4 of these $\Delta(\mathbf{k}) = 0$, as is true on the 16-site system. s-wave solutions can more easily be found in small systems for short-range interactions. In such a case $V_{\mathbf{k},\mathbf{k}'} \approx$ const, $\Delta(\mathbf{k}) \approx$ const, and all $\mathbf{k}$ points contribute. It is not necessary to build up the kind of constructive interference which d-wave solutions require.

In conclusion, our VMC calculations show that d-wave superconductivity can be supported in the two-dimensional t-J model for square, finite-sized systems as long as the lattice size is large enough. The d-wave pairing state does conclusively minimize the ground-state energy for lattice sizes on the order of or greater than 100 sites for a variational gap parameter ψ_d of $0.2 \pm 0.1t$. Results of calculations done on a 226-site system confirm that, for $\delta \approx 0.125$, assuming a lattice size of 100 sites was large enough to "lock into" this $\psi_d \approx 0.2t$ result. We wish to point out here that this result is physically reasonable. As cited in Sec. I, experiment suggests that $t \approx 400$ meV

in $YBa_2Cu_3O_7$, which would make $\psi_d = 80 \pm 40$ meV. Furthermore, the condensation energy from Fig. 2(c) is $E_c \equiv E_G(\psi_d = 0) - E_G(\psi_d = 0.2t) = 0.005 \pm 0.002t$ per hole, and this would be $E_c = 2.77 \times 10^{18}$ eV/cm^3 assuming two CuO_2 sites per unit cell and $t = 400$ meV.[28] Now, a simple estimate of $E_c = H_{c1}H_{c2}/8\pi$ yields $E_c = 1.99 \times 10^{18}$ eV/cm^3 for the approximate experimental values of $H_{c1} = 100$ G and $H_{c2} = 5 \times 10^5$ G. These values of the condensation energy are certainly in reasonable agreement with one another. Comparison with the QMC investigations suggests that the contradiction between the QMC results and our VMC results may be due to differences of model and limitations of temperature and lattice size of the QMC study. We believe that for the restricted task of determining whether there is a superconducting ground state for the minimal model in the experimental range of parameters, VMC is superior to QMC. The latter is restricted to rather high temperatures, moderate interaction strength, and small lattice sizes.

IV. VMC RESULTS AND COMPARISON OF OTHER PAIRING STATES

In addition to the d-wave calculations presented in the previous section, further VMC calculations were made assuming different pairing states in the t-J model. The purpose of investigating other pairing states was threefold. First, we want to find which state best minimized the energy, thus showing which of the pairing states is the best candidate ground state of the group. Second, using the same finite-sized lattices as before, we were interested in seeing at what system size this best candidate ground state was able to overcome finite-size effects and minimize the energy expectation value for some nonzero variational gap parameter, thus showing a favoring of that pairing state over the normal state. Third, previous calculations had indicated that at hole densities $\delta > 10\%$, mixing of s-wave and d-wave states might be preferred.[21] The pairing states investigated are the extended s, $s + d$, and $s + id$ waves. The corresponding gap functions are defined as follows:

$$\Delta_{ES}(\mathbf{k}) \equiv \psi_{ES}(\cos k_x + \cos k_y), \tag{14}$$

$$\Delta_{s+d}(\mathbf{k}) \equiv \psi_s(\cos k_x + \cos k_y) + \psi_d(\cos k_x - \cos k_y), \tag{15}$$

$$\Delta_{s+id}(\mathbf{k}) \equiv \psi_s(\cos k_x + \cos k_y) + i\psi_d(\cos k_x - \cos k_y). \tag{16}$$

Here ψ_{ES} is a variational gap parameter, which varied from 0.0 to $1.0t$ for the extended s-wave state just as ψ_d was varied for the d-wave state. For the mixed $s + d$ and $s + id$ states, the parameters ψ_{s+d} and ψ_{s+id} (both defined as $\sqrt{\psi_s^2 + \psi_d^2}$) were varied from 0.0 to $1.0t$. In most calculations we set $\psi_s = \psi_d$. The same hole densities and lattice sizes were used as described in the previous section.

Figures 5(a), 5(b), and 5(c) show the energy vs gap parameter calculations for the 16-site lattice at hole densities of 0.125, 0.250, and 0.375, respectively. Included are the previous d-wave results along with s-, $s + d$-, and $s + id$-wave calculations. The most striking feature of these curves is that for the $\delta = 0.125$ and 0.250 cases, the various wave states do not converge to the same normal-state energies as $\psi \to 0$. It is expected, as properly shown in the $\delta = 0.375$ case, that as $\psi \to 0$, the various gap functions should also go to zero, and the normal-state energy calculated should be the same for all states tested. This discrepancy demands some elaboration. It can be seen in Eq. (11) that there is some ambiguity in how $a(\mathbf{k})$ is defined when $\Delta(\mathbf{k}) = 0$ and $\xi_{\mathbf{k}} \leq 0$. This problem is magnified when the gap function vanishes over a large fraction of the points in k space. This has already been demonstrated by $\Delta_d(\mathbf{k})$ in Fig. 4 for the $N = 16$ case. As a result of this arbitrariness in defining $a(\mathbf{k})$ at certain node points, some of the energy curves shown in Figs. 5(a), 5(b), and 5(c) have differing normal-state limits and are shifted with respect to one another. It will next be shown that these discrepancies neither cause qualitative problems nor persist as the system size is increased and the fraction of node points decreases.

It turns out that this problem of different normal-state limits does indeed go away as the size of the lattice increases. Figures 6(a), 6(b), and 6(c) show the energy vs gap parameter results for a 64-site lattice, assuming the same parameters used in the 16-site calculations. The discrepancy of normal-state energies for certain hole densities is still apparent, but it is clear that the curves are converging much better than they did in the 16-site case. The discrepancy in energies becomes still smaller for even larger systems, and in fact, this investigation was the first time we even noticed this particular problem resulting from the ambiguity of $a(\mathbf{k})$ when $\Delta(\mathbf{k}) = 0$ and $\xi_{\mathbf{k}} \leq 0$. Our previous investigations have been typically done on lattice sizes of 82 sites or more. Until now, any discrepancies in normal-state ($\psi \to 0$) calculations have been within statistical noise.

Similar calculations as those already shown for the 16- and 64-site systems were done on 26-, 36-, 50-, 82-, and 100-site lattices as well. There are three results important to this investigation which are presented in the following remarks. First, the $s + id$ energy calculations are consistently lower than those of the pure s and the pure d waves for most hole densities and lattice sizes investigated. This is consistent with earlier VMC calculations which showed that for hole densities above 0.10, the $s + id$-wave state was preferred over the d-wave state, and the d-wave state was preferred for $\delta < 0.10$.[21] The second result of note from these various wave-state VMC calculations is that the $s + id$-wave calculations show a conclusive preference of a superconductive pairing state over the normal state for even smaller systems than the 100-site lattice result for the d-wave state. Figures 7(a) and 7(b) show the ground-state energy vs variational gap parameter results for the $s + id$ wave for all the finite sizes used and at a hole density of approximately 0.125. For the $s + id$ wave, the minimum for the 36-site calculations corresponds to a gap parameter ψ_{s+id} of $0.2 \pm 0.1t$, where comparison with Fig. 2(a) shows that at 36 sites, the minimum is at $\psi_d = 0$ for d-wave states. Figure 7(c) shows the $s + id$-wave results for $\delta \approx 0.25$. Here it can be

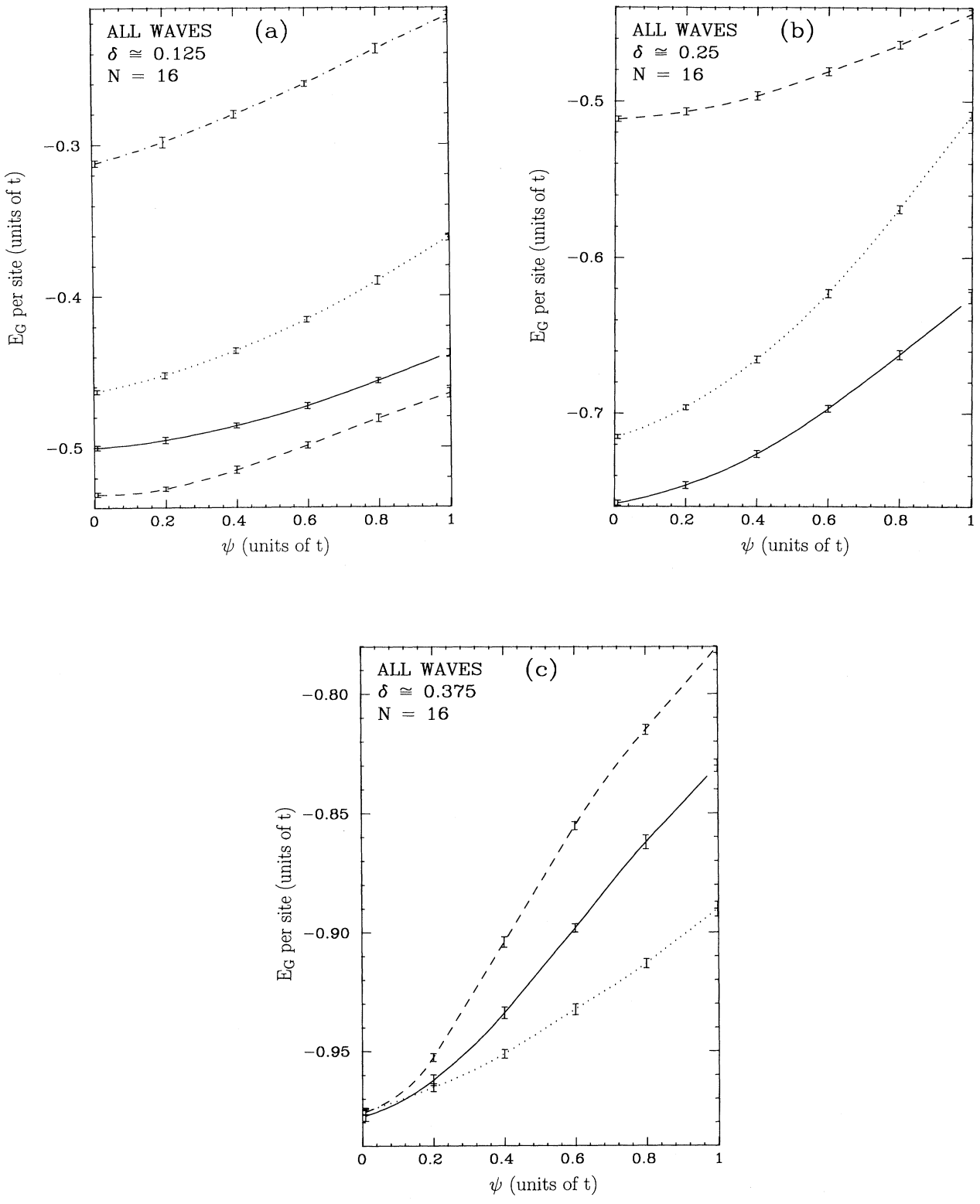

FIG. 5. Shows the calculated energy expectation value vs variational gap parameters for the s-wave (dotted line), the d-wave (dashed line), the $s+d$ (dot-dashed line), and the $s+id$ states (solid line), where ψ_{s+d} and $\psi_{s+id} = \sqrt{\psi_s^2 + \psi_d^2}$. These calculations were done on a 16-site lattice with (a) $\delta = 0.125$, (b) $\delta = 0.250$, and (c) $\delta = 0.375$. Note in (c) that all four states converge to the same normal-state energy as their respective ψ's $\rightarrow 0$, whereas there are different limits for (a) and (b). For the $s+d$ and $s+id$ waves $\psi_s = \psi_d$.

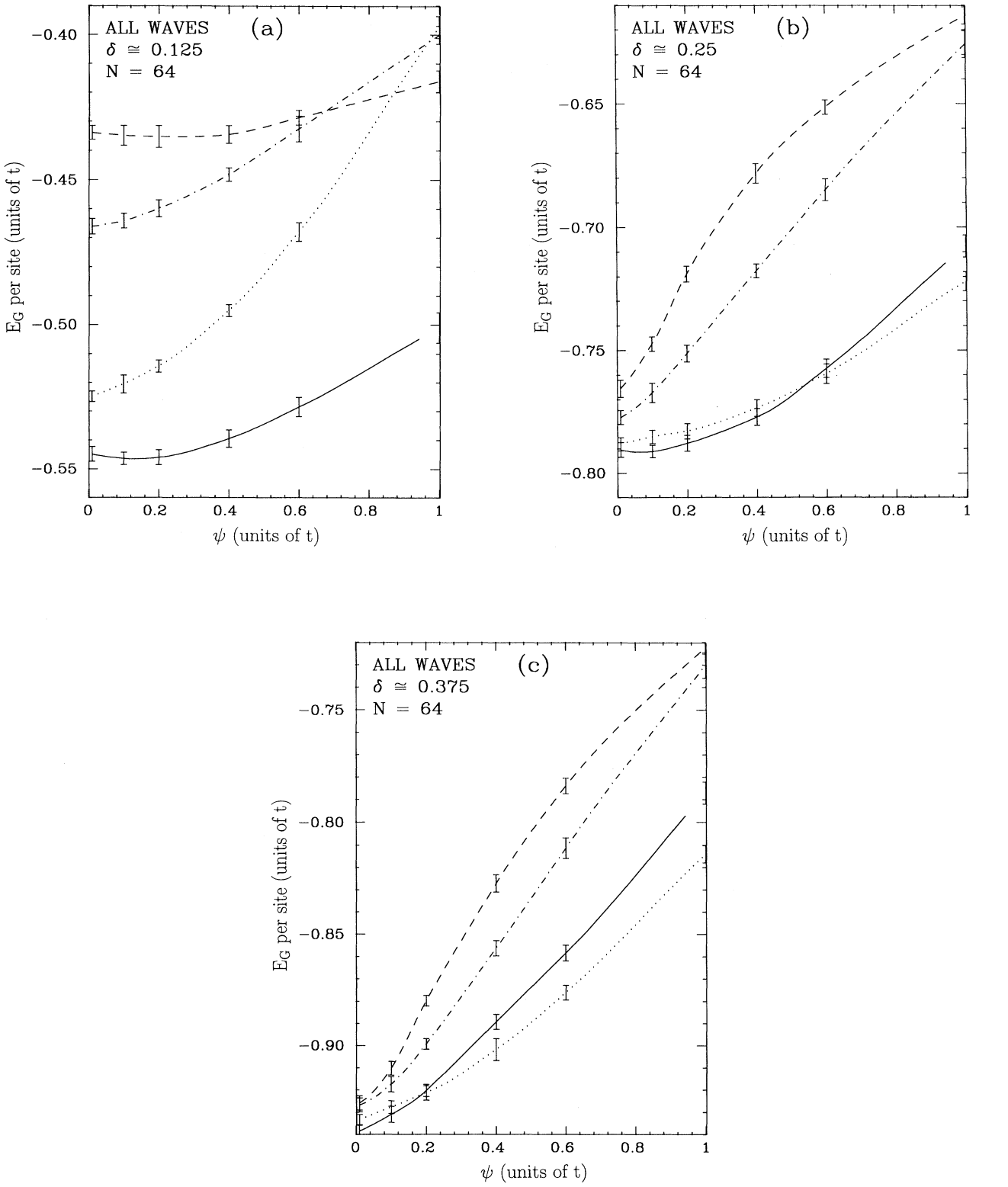

FIG. 6. Shows the calculated energy expectation value vs variational gap parameters for the s-wave (dotted line), the d-wave (dashed line), the $s+d$ (dot-dashed line), and the $s+id$ states (solid line), where ψ_{s+d} and $\psi_{s+id} = \sqrt{\psi_s^2 + \psi_d^2}$. These calculations were done on the 64-site lattice for (a) $\delta = 0.125$, (b) $\delta = 0.250$, and (c) $\delta = 0.375$. Note the varying $\psi \to 0$ limits for each hole density δ are much closer than in the 16-site cases of Fig. 5.

seen that for 64 sites, the $s + id$-state wave is preferred over the normal state with a gap parameter $\psi_{sd} \approx 0.1t$. (This minimum, however, is on the order of the statistical uncertainty of the energies calculated, but further calculations confirm there is indeed a minimization of energy below normal-state energy here.) Comparison with Figs. 3(a) and 3(b) shows that while the d-wave pairing is not preferred over the "normal state" ($\psi_d = 0$) at $\delta \approx 0.25$

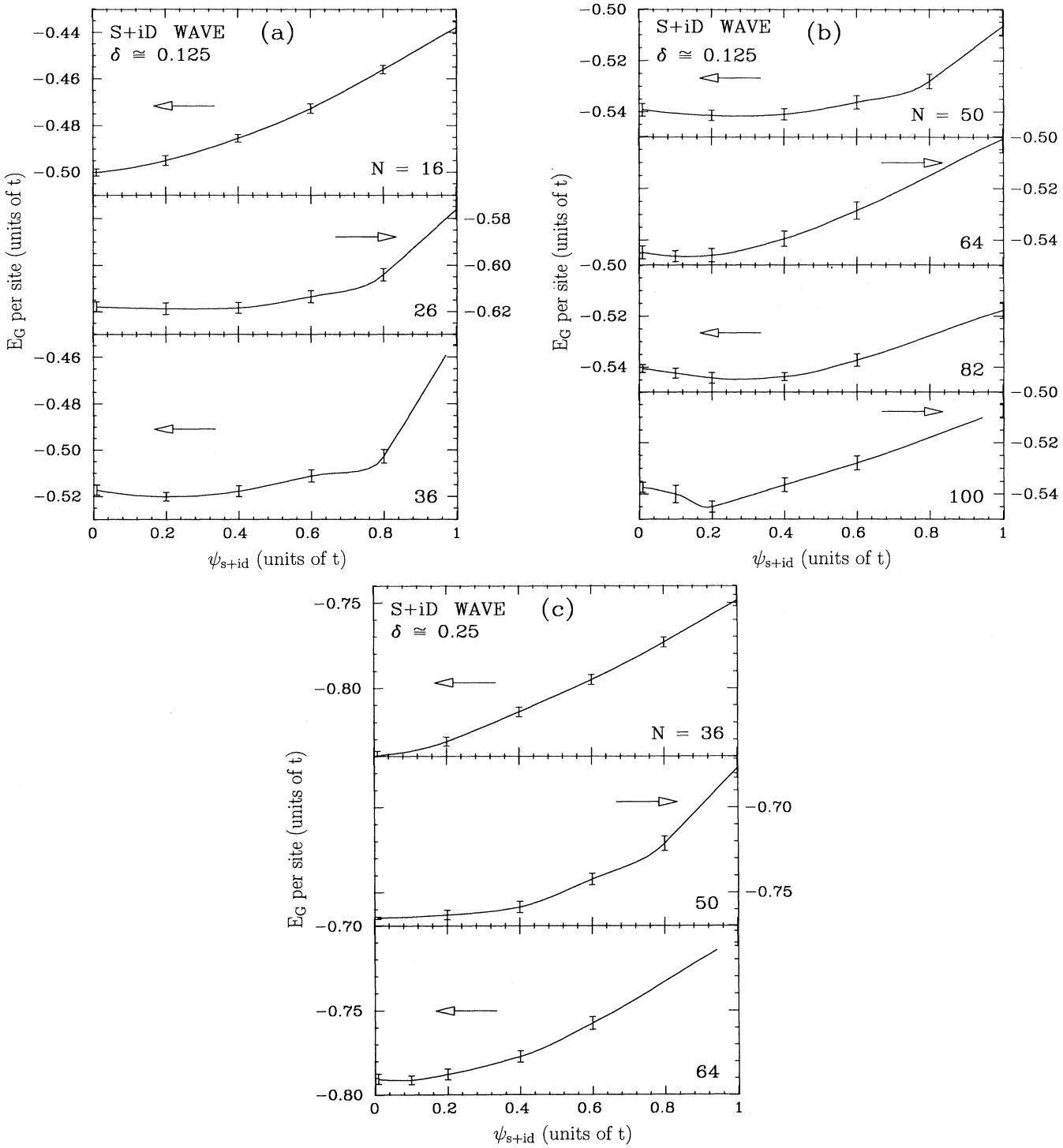

FIG. 7. Shows the calculated energy expectation value vs variational gap parameter ψ_{s+id} for the $s + id$ wave for $\delta \approx 0.125$ on (a) 16-, 26-, and 36-site lattices and (b) 50-, 64-, 82-, and 100-site lattices. (c) Shows similar calculations for $\delta \approx 0.250$ on 36-, 50-, and 64-site lattices.

for *any* of the lattice sizes investigated, the $s+id$ state is preferred at this size of 64 sites (and above). According to our VMC calculations, the $s+id$ state not only is preferred over the d-wave state at these hole densities, but it is also able to overcome finite-size effects at even smaller lattice sizes than the d-wave state. This is in agreement with the discussion of the previous section.

The third and final result of this investigation is that, for the cases where there were no normal-state discrepancies in energies for a given configuration, or where such discrepancies were negligible, the $s+d$- and $s+id$-wave results were essentially identical. Further study of this result showed no differences in energy calculations over a wide range of parameters. Figure 8(a) shows one such study, where the results of VMC energy calculations for a mixed state of changing phase are presented. A 122-site system with $\delta \approx 0.30$ was used. Here, the gap function was assumed to be

$$\Delta_\varphi(\mathbf{k}) \equiv \Delta_{ES}(\mathbf{k}) + e^{i\varphi}\Delta_d(\mathbf{k}), \tag{17}$$

where $\Delta_{ES}(\mathbf{k})$ and $\Delta_d(\mathbf{k})$ are defined in Eqs. (14) and (12), respectively. The variational gap parameters were both fixed at 0.106t such that $\psi_\varphi = \sqrt{\psi_{ES}^2 + \psi_d^2}$ was fixed at $0.15t$, and φ was varied from 0 (corresponding to the $s+d$ wave) to $\frac{\pi}{2}$ ($s+id$ wave). Clearly, there is essentially no variation in these energy calculations shown in Fig. 8(a). Therefore, there are no distinguishable differences between $s+d$-, $s+id$-, and $s+e^{i\varphi}d$-wave energy calculations in this VMC method. For the Ginzburg-Landau theory of Sec. II, this implies that $\beta_p \approx 0$ in Eq. (2).

Next we study the effect of the relative weighting of the two variational gap parameters for the $s+id$ state. Figure 8(b) shows the calculated energy expectation value for the $s+id$ wave on a 122-site lattice with $\delta \approx 0.30$. Here, ψ_s and ψ_d were varied such that $\psi_{s+id} = \sqrt{\psi_s^2 + \psi_d^2} = 0.15t$. It is apparent that the lowest energy calculated indeed corresponds to the $\psi_s = \psi_d$ assumption made throughout this entire small-lattice-size investigation. This corresponds to Landau parameters defined in Sec. II which satisfy $|\beta_s/\alpha_s T_s| \approx |\beta_d/\alpha_d T_d|$ and $\beta_{sd} < 2\beta_s$, $\beta_{sd} < 2\beta_d$. Surprisingly, however, as long as neither ψ_s nor ψ_d were set too small (which would correspond to a more d-wave-like and a more s-wave-like state, respectively), the energy calculated changed very little.

In final summary of all the VMC numerical calculations, it has been shown that the $s+id$ state does indeed stand as a strong candidate superconducting ground state for the parameters investigated, being superior to the d wave at the hole densities used throughout this investigation. The main results of this study are again listed here in brief.

(1) The mixed $s+id$ and $s+d$ waves are energetically preferred over the s and d waves for the hole densities studied ($\delta \approx 0.125$, 0.250, and 0.375). This is consistent with an earlier study which showed d-wave pairing at $\delta < 0.1$.

(2) The $s+id$ wave is able to overcome finite-size effects at smaller lattice sizes than the d wave.

(3) The energy of the $s+e^{i\varphi}d$ state is almost independent of the relative phase φ.

(4) Small variation in the weighting of the s- and d-wave parts of the $s+id$ wave causes little change in the $s+id$-wave energy calculations. This is not the case if either the s- or d-wave parts are allowed to approach zero.

(5) Ambiguity in how $a(\mathbf{k})$ is defined for $\Delta(\mathbf{k}) = 0$ and $\xi_\mathbf{k} \leq 0$ can result in discrepancies in normal-state ($\psi \to 0$) energy limits. For the smaller system sizes these discrepancies can be quite large due to the large fraction of node points where $\Delta(\mathbf{k})$ vanishes. For larger systems,

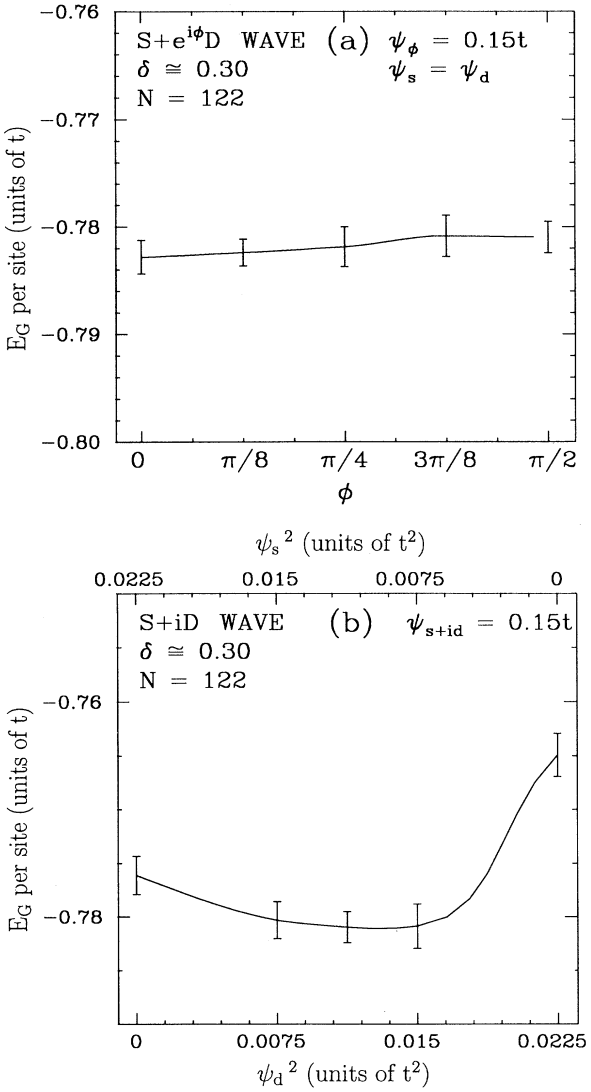

FIG. 8. (a) Shows the calculated energy expectation value vs variational phase parameter φ for the $s+e^{i\varphi}d$ wave. $\varphi = 0$ corresponds to an $s+d$ wave and $\varphi = \frac{\pi}{2}$ to an $s+id$ wave. $\psi_\varphi = \sqrt{\psi_s^2 + \psi_d^2}$, where $\psi_s = \psi_d = 0.160t$. (b) Shows calculated energy expectation value vs variational gap parameters ψ_s^2 and ψ_d^2 for the $s+id$ wave. Here, $\psi_{s+id} = \sqrt{\psi_s^2 + \psi_d^2} = 0.15t$. $\psi_d = 0$ corresponds to a pure s-wave state, $\psi_s = 0$ to a pure d-wave state. Calculations for both (a) and (b) were done on a 122-site lattice with $\delta = 0.30$.

these differences become negligible.

(6) The three-site term of Eq. (1) is very important for determining the ground state, and tends to favor the s-wave component.

V. DENSITY OF STATES, PENETRATION DEPTH

We turn now to calculation of experimentally measurable properties of the $s + id$ state. These generally involve measurements at finite temperatures and finite frequencies. Such quantities are currently beyond the range of the VMC method. Accordingly, we perform the simplest calculations possible (random-phase approximation) on a simple tight-binding model of electron dynamics. There is no guarantee that these calculations, which essentially use weak-coupling methods, are consistent with the strong-coupling ideas of Secs. III and IV. There simply appears to be no alternative at the present time.

The density of states (DOS) is one of the most important quantities in condensed-matter physics because it is related to many thermodynamic as well as transport properties. The DOS of a superconducting state can be measured directly by the tunneling experiment. Theoretically, the DOS is proportional to the imaginary part of the single-particle Green's function,

$$D(\omega) = -\frac{1}{\pi}\mathrm{Im}\sum_{\mathbf{p}} G(\mathbf{p},\omega). \tag{18}$$

For a superconducting state,

$$G(\mathbf{p},\omega) = \frac{u_p^2}{\omega - E_p + i\Gamma} + \frac{v_p^2}{\omega + E_p + i\Gamma}. \tag{19}$$

Here $E_p^2 = |\Delta(\mathbf{p})|^2 + \xi_{\mathbf{p}}^2$, $\xi_{\mathbf{p}} = \epsilon(\mathbf{p}) - \mu$, $u_p^2 = \frac{1}{2}(1+\xi_p/E_p)$, and $v_p^2 = \frac{1}{2}(1-\xi_p/E_p)$ are all the standard notations. Γ is the broadening due to the inelastic scattering, which is twice the inverse quasiparticle lifetime.

In Figs. 9(a), 9(b), and 9(c) we show the calculated DOS of the s-wave [$\Delta(\mathbf{k}) = \psi_s = \mathrm{const}$], d-wave [Eq. (12)], and $s + id$ states,

$$\Delta(\mathbf{k}) = \psi_s + i\psi_d(\cos k_x a - \cos k_y a). \tag{20}$$

The DOS of the s-wave state is $(E-\psi_s)^{-1/2}$ divergent at $E = \psi_s + 0$ and is zero at $E < \psi_s$ in the limit $\Gamma \to 0$, while the DOS of the d-wave state is logarithmically divergent at the maximum gap, remains finite inside the maximum gap, and goes to zero linearly as $E \to 0$. The DOS of the $s + id$ state is logarithmically divergent at the maximum gap, has a kink on the minimum gap, and becomes zero inside the minimum gap ψ_s.

As we have already seen, one of the obvious differences between the s-wave and the d-wave states is whether there are any nodes in the gap function. This will affect the low-temperature behavior of many physical quantities. One of them is the electromagnetic penetration depth. The penetration depth measurement is in principle a clean probe of the superconducting state because it directly measures the superfluid density. By looking at the asymptotic low-temperature behavior—whether it is exponential or power law—one can tell if there are any nodes in the gap. Apparently among s-wave, d-wave, and $s + id$ states, both the s-wave and $s + id$ states have nodeless gap functions and the penetration depth should have an exponential temperature dependence in the low-temperature region, while the d-wave state predicts a linear temperature dependence in the low-T region. We emphasize that above predictions are only valid in the absence of impurities (or disorder).

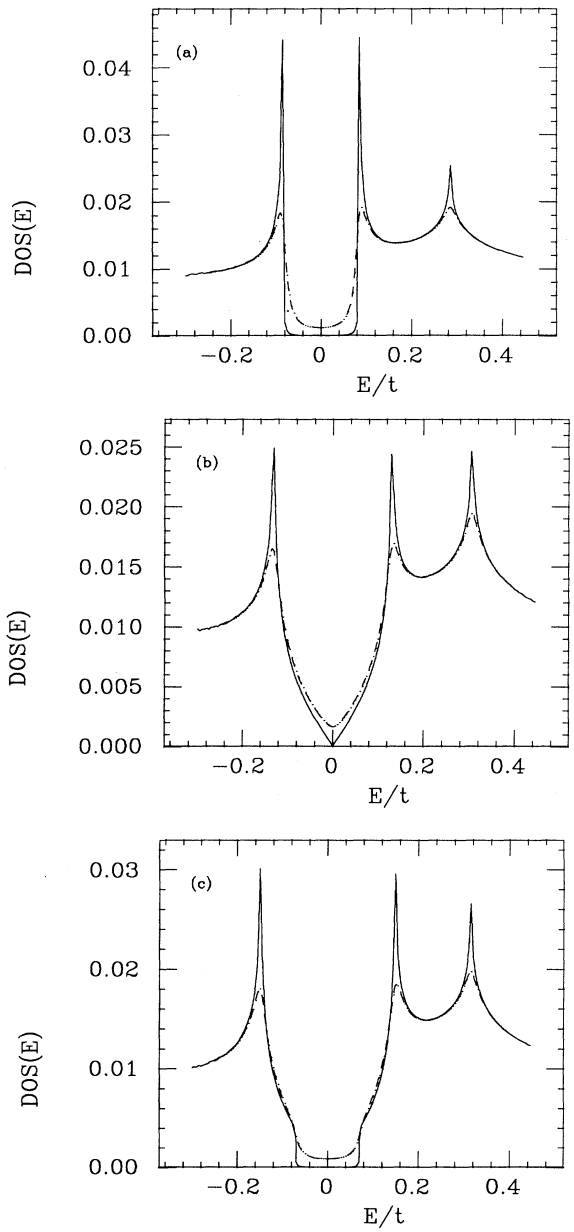

FIG. 9. Shows the calculated DOS of (a) s-wave [$\psi_s(0) = 1.76k_BT_c$], (b) d-wave [$\psi_d(0) = 1.5k_BT_c$], and (c) $s+id$ states [$\psi_s(0) = \psi_d(0) = 1.5k_BT_c$] for $\Gamma = 0.2k_BT_c$ (dashed line) and $\Gamma = 0.01k_BT_c$ (solid line), respectively. The parameters used in the calculation are $t = 20k_BT_c$, $U = 2t$.

Experimentally, the penetration depth can be measured in several ways: magnetization of thin crystals, muon spin rotation (μSR), kinetic inductance, phase velocity of a microwave signal propagating along a thin film, and others. Earlier, some groups have used the s-wave state to interpret their data.[29,30] Later analysis of the surface impedance data of Fiory *et al.*[30] by Annett, Goldenfeld, and Renn[31] found that $\delta\lambda_{ab}(T) = \lambda_{ab}(T) - \lambda_{ab}(0) \propto T^2$ in epitaxial $YBa_2Cu_3O_7$ films. More recently, Pond *et al.*[32] found that their phase velocity data can be fit by both the s-wave pairing and the empirical form

$$\lambda(T) = \frac{\lambda(0)}{\sqrt{1-(T/T_c)^2}}. \tag{21}$$

The latter seems to give a little bit better fit. This empirical form was also found to be in good agreement with the experimental data of Anlage *et al.*[33] who measure the phase velocity of a microwave signal propagating along a thin film of a high-T_c superconductor.

To summarize the current status, recent experiments show that the temperature dependence of the magnetic penetration depth is not consistent with a simple scaled weak-coupling BCS temperature dependence. The experimental data in the low-temperature region ($0.1T_c < T < 0.5T_c$) can be fit by either an anisotropic gap function with a small but nonzero minimum gap or a power-law T^2 dependence. The former is in agreement with the $s + id$ gap function, while the latter would indicate nodes in the gap function. The question remains whether the experiments are in the *asymptotic* low-temperature regime. If the T^2 dependence is confirmed to be the true low-temperature behavior, it certainly lends support to the gapless superconducting order parameter, but it is not a straightforward confirmation for the d-wave case, at least not in the clean limit where the d wave predicts a linear T dependence. Note that the clean limit is not an unreasonable limit for high-T_c materials because of their short coherence length. Recently, Prohammer and Carbotte[34] studied the effect of impurities on the penetration depth in d-wave superconductors. They find that by introducing so-called unitary scattering, one can produce the T^2 near $T = 0$ in the d-wave case. They also show that Born approximation of impurity scattering does not change the linear T behavior of the London penetration depth in d-wave superconductors. But there is a question whether the unitary approximation can be applied to high-T_c superconductors. Unlike in the heavy-fermion systems where unitary scattering is proposed to be realized due to the underlying Kondo lattice, the assumption of unitary scattering in high-T_c superconductors is less justified.

Experimentally the angular dependence of the gap may be measured rather directly by angle-resolved photoemission. In particular recent measurements in $Bi_2Sr_2CaCu_2O_8$ show a gap $\Delta(10) = 24 \pm 3$ meV along the k_x axis and a gap $\Delta(11) = 18 \pm 3$ meV along the $k_x = k_y$ line, so that $\Delta(10)/\Delta(11) \approx 1.33$.[35] The $s + id$ state proposed here [Eq. (20), $\psi_s = \psi_d$] would give $\Delta(10)/\Delta(11) = 1.92$ at $\delta = 0.30$.

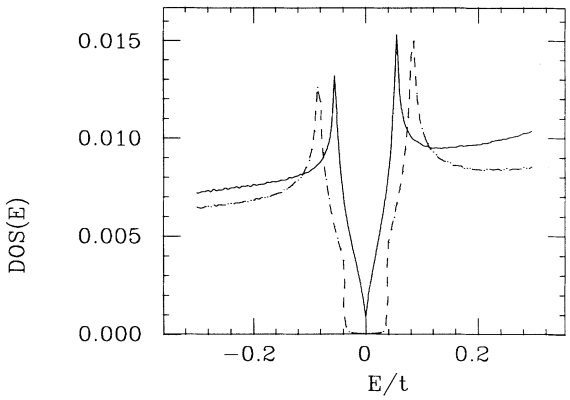

FIG. 10. Shows the calculated DOS of an extended s-wave state for doping $\delta = 0.24$ (dashed line) and $\delta = 0.14$ (solid line), respectively. The parameters used in the calculation are $t = 20k_BT_c$, $t_2 = 0.15t$, $U = 2t$, $\psi_{ES}(0) = 5.0k_BT_c$.

Finally we comment on the extended s-wave state. We have used the tight-binding single-particle dispersion $\epsilon_{\mathbf{k}} = -2t(\cos k_x + \cos k_y)$ in our discussion above. In this case, extended s-wave $\Delta(\mathbf{k}) = \psi_{ES}(\cos k_x + \cos k_y)$ is essentially equivalent to the usual isotropic s-wave state $\Delta(\mathbf{k}) = \psi_s = \text{const}$ because the extended s-wave state is also constant on the Fermi surface. To make the extended s-wave state anisotropic, one has to choose some dispersion relation other than the tight-binding one, for example, by including next-nearest-neighbor hopping,

$$\epsilon_{\mathbf{k}} = -2t(\cos k_x + \cos k_y) - 4t_2 \cos k_x \cos k_y. \tag{22}$$

In Fig. 10, we show the DOS of the extended s-wave state at 14% and 24% doping. We can see the DOS of some extended s-wave state is very similar to that of the $s + id$ state, while the other looks like a gapless d-wave state. As we discussed earlier in Sec. II, the most nontrivial property of the d-wave state is that the gap function changes sign when rotated by 90°. This property is not manifest in the DOS because it depends on the square of the gap function only. There are, however, some other physical quantities, such as the nuclear spin-lattice relaxation time $1/T_1$, which are sensitive to the phase information in the gap function. One can use those properties to distinguish extended s-wave, d-wave, and $s + id$ states. We shall discuss that in the next section.

VI. NUCLEAR MAGNETIC RESONANCE (NMR)

In this section we calculate the nuclear spin-lattice relaxation time $1/T_1$ and Knight shift of $YBa_2Cu_3O_7$ below the critical temperature using various pairing states including s-wave, d-wave, and $s + id$ states and compare them with the currently available experimental data. We concentrate on $YBa_2Cu_3O_7$ because that is where most experimental studies were done.[36] Our calculation can be easily extended to other high-T_c superconductors because the essential ingredient is the CuO_2 plane which is the trademark of high-T_c superconduc-

tors. Theoretically, the normal-state NMR data have been studied by Mila and Rice (MR),[9] Millis, Monien, and Pines (MMP),[10] Bulut *et al.*,[37] and others.[38] Monien and Pines,[39] Lu,[40] Bulut and Scalapino[41] have also tried to fit the superconducting-state NMR data using either s-wave or d-wave pairing. Following MR and MMP, we use the electron-nuclei coupling Hamiltonian of the CuO_2 plane,

$$H^{e\text{-}n} = {}^{63}\mathbf{I}_n \cdot A \cdot \mathbf{S}_n + B \sum_{\tau} {}^{63}\mathbf{I}_n \cdot \mathbf{S}_{n+\tau} + C \sum_{\tau'} {}^{17}\mathbf{I}_n \cdot \mathbf{S}_{n+\tau'}. \quad (23)$$

Here again we use the Zhang-Rice one-band model of the CuO_2 plane and assume that the spins reside on the Cu sites.[6] τ and τ' label the four unit cells to Cu site n and the two nearest Cu sites of the planar O, respectively. A, B, and C are the hyperfine coupling constants. A is the direct hyperfine tensor.

The nuclear spin-lattice (also called longitudinal) relaxation time $1/T_1$ is related to the imaginary part of the susceptibility $\chi(\mathbf{q},\omega)$,[42]

$$T_1^{-1} = (\gamma_n^2 k_B T/2\mu_B^2) \lim_{\omega\to 0} \sum_{\mathbf{q}} G(\mathbf{q}) \mathrm{Im}\chi(\mathbf{q},\omega)/\omega. \quad (24)$$

Here $G(\mathbf{q})$ is the hyperfine coupling between the electronic spin and the nuclear spin which has gyromagnetic ratio γ_n. Using the above electron-nuclei coupling Hamiltonian, one finds that on the Cu(2) site,

$$G_a(\mathbf{q}) = [A_{zz} + 2B(\cos q_x + \cos q_y)]^2 + [A_{xx} + 2B(\cos q_x + \cos q_y)]^2, \quad (25)$$

$$G_c(\mathbf{q}) = 2[A_{xx} + 2B(\cos q_x + \cos q_y)]^2, \quad (26)$$

for the magnetic field parallel to the a and c axes, respectively. On the O(2,3) site,

$$G_O(\mathbf{q}) = 4C^2 \cos^2(q_{y,x}/2). \quad (27)$$

This form of $G(q)$ has been used successfully by MR and MMP to calculate the NMR properties of $YBa_2Cu_3O_7$ above T_c.[9,10] In the rest of the paper, we adapt the parameter values $A_{xx} = B = -0.25A_{zz}$ from MR's and MMP's calculation on the normal state of $YBa_2Cu_3O_7$.

We calculate $\chi(\mathbf{q},\omega)$ using the random-phase approximation (RPA),[43]

$$\chi(\mathbf{q},\omega) = \frac{\chi_0(\mathbf{q},\omega)}{1 - U\chi_0(\mathbf{q},\omega)}. \quad (28)$$

Here U is the effective Hubbard interaction and χ_0 is the "noninteracting" spin susceptibility of a superconducting state ("bare bubbles"),

$$\chi_0(\mathbf{q},\omega) = \sum_{\mathbf{p}} [1 - n_F(E_{p_+}) - n_F(E_{p_-})]F_1 + [n_F(E_{p_+}) - n_F(E_{p_-})]F_2, \quad (29)$$

where

$$F_1 = \frac{1}{4}\left(1 - \frac{\xi_{p_+}\xi_{p_-} + \Delta(\mathbf{p}_+)\Delta^*(\mathbf{p}_-)}{E_{p_+}E_{p_-}}\right)\left[\frac{1}{\omega + E_{p_+} + E_{p_-} + i\Gamma} - \frac{1}{\omega - E_{p_+} - E_{p_-} + i\Gamma}\right],$$

$$F_2 = \frac{1}{2}\left(1 + \frac{\xi_{p_+}\xi_{p_-} + \Delta(\mathbf{p}_+)\Delta^*(\mathbf{p}_-)}{E_{p_+}E_{p_-}}\right)\left[\frac{1}{\omega - E_{p_+} + E_{p_-} + i\Gamma}\right].$$

Here $E_p^2 = |\Delta(\mathbf{p})|^2 + \xi_{\mathbf{p}}^2$, $\xi_{\mathbf{p}} = \epsilon(\mathbf{p}) - \mu$, $\mathbf{p}_\pm = \mathbf{p} \pm \mathbf{q}/2$, and $n_F(E)$ is the Fermi distribution function. The F_1 term corresponds to pair breaking and forming, and the F_2 term corresponds to the scattering of thermally excited (Bogoliubov) quasiparticles. Although the F_2 term usually dominates the spin dynamics when the pair-breaking scattering rate Γ is small, the F_1 term is not negligible for larger Γ. We always keep both the F_1 and F_2 terms in our calculation.

The temperature dependence of the scattering rate $\Gamma(T)$ is not clear at the present stage. We assume a simple form $\Gamma(T) = \Gamma_0 + \Gamma_1(T/T_c)^n$ with $\Gamma_0 = 0.1T_c$, $\Gamma_1 = 0.4T_c$, and $n = 2$ in our calculation. We have tried various parameter values and find that the usage of different parameter values with the constraint that Γ at $T = T_c$ does not exceed $0.5T_c$ does not change our results in any qualitative way. To calculate $1/T_1$, one must also know the temperature dependence of the gap function. In our calculation, we use the standard approximate form $\psi_s(T) = \psi_s(0)\tanh(1.74\sqrt{\frac{T_c}{T} - 1})$, which fits the numerical solution of the weak-coupling BCS gap equation very well. We also use a similar formula for $\psi_d(T)$ for simplicity. A more accurate form of $\psi_d(T)$ can be obtained by solving the d-wave gap equation.

In Fig. 11(a) we show the calculated $1/T_1$ of Cu(2) using s-wave, d-wave, and $s + id$ states. We also plot the experimental result of Takigawa, Smith, and Hults for comparison.[44] Figure 11(b) is the calculated $1/T_1$ of O(2,3) and the experimental data.[45,46] We use a tight-binding single-particle dispersion $\epsilon(\mathbf{p}) = -2t(\cos p_x + \cos p_y)$, where t is the nearest-neighbor hopping integral. We choose $U = 2t$ and the filling factor n=0.86 following Bulut and Scalapino.[41] We have tried various parameter

values $\psi_s(T=0)$ and $\psi_d(T=0)$ in our calculation and the parameter values we used in Fig. 11 represent one of the best choices as far as fitting the relaxation rate of Cu(2) and O(2,3) is concerned. One can see from Fig. 11 that for a reasonable scattering rate Γ around $0.5T_c$, the Hebel-Slichter peak is absent even for an s-wave state. So the absence of the coherent peak in the $1/T_1$ measurement is not necessarily against the conventional s-wave pairing.[47]

The temperature dependence of the anisotropy ratio of Cu(2), $(1/T_1)_a/(1/T_1)_c$, has a strange behavior below T_c: It decreases first as one lowers the temperature, and then turns around near $T=0.8T_c$, and starts to increase as the temperature is lowered further (cf. Fig. 12). In Fig. 12(a), we plot the calculated anisotropy ratio of Cu(2), $(1/T_1)_a/(1/T_1)_c$, as a function of temperature for s-wave pairing states. The experimental result of Takigawa, Smith, and Hults[44] is also shown for comparison. We can see that the s-wave state fails to produce the upturn in the low-temperature region of the experimental data.[40] Figure 12(b) shows calculated anisotropy ratio for the d-wave and the $s+id$ states; we find that both of them agree with the experiment qualitatively. This qualitative feature of the calculation is independent of the choice of $\psi_s(0)$ and $\psi_d(0)$ within a reasonable range. The reason is that $(1/T_1)_a$ and $(1/T_1)_c$ have different spectral weights $G(\mathbf{q})$ for different momentum transfer $\mathbf{q}$. For s-wave states, the coherence factor (of the F_2 term)

$$c(\mathbf{p},\mathbf{q}) = 1 + \frac{\xi_{p+q}\xi_p + \Delta(\mathbf{p}+\mathbf{q})\Delta^*(\mathbf{p})}{E_{p+q}E_p}$$

is almost independent of $\mathbf{q}$ when $\mathbf{p}$ is near the Fermi surface and contributes equally to $(1/T_1)_a$ and $(1/T_1)_c$.[40] For d-wave and $s+id$ states, on the other hand, the coherence factor does depend on $\mathbf{q}$, varying from 2 for small $\mathbf{q}$ to less than 1 for some large $\mathbf{q}$. This $\mathbf{q}$ dependence of the coherence factor, together with the difference in spectral weight of $(1/T_1)_a$ and $(1/T_1)_c$, is responsible for the temperature dependence of the anisotropy ratio observed in the experiment.

Next we consider the ratio of the relaxation rate of Cu(2) and O(2,3), $(1/T_1)_c/(1/T_1)_O$, which provides yet another test for possible theories. In Fig. 13 we show

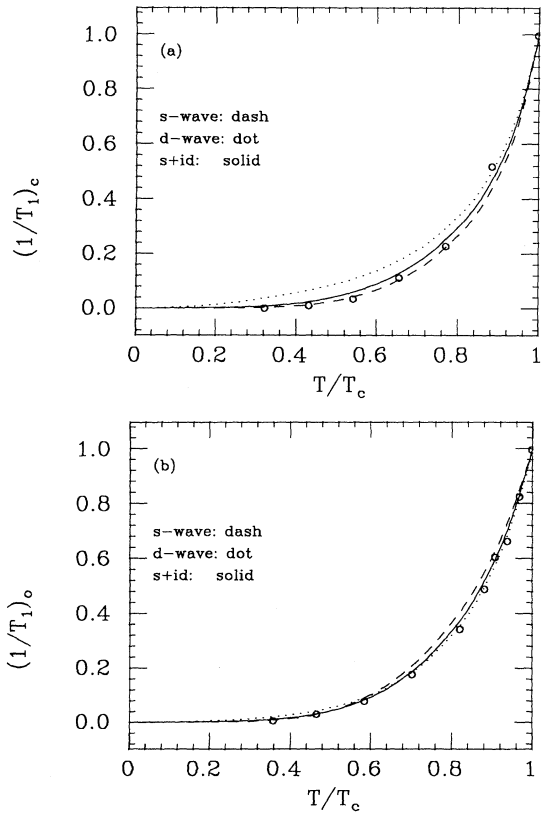

FIG. 11. Shows the calculated $1/T_1$ at (a) Cu(2) and (b) O(2,3) as a function of temperature for s-wave [$\psi_s(0) = 2.5k_BT_c$, dashed line], d-wave [$\psi_d(0) = 1.8k_BT_c$, dotted line], and $s+id$ states [$\psi_s(0) = \psi_d(0) = 1.5k_BT_c$, solid line]. Here $1/T_1$ is normalized to its value at $T=T_c$. The parameters used in the calculation are $t = 20k_BT_c$, $U=2t$, and $\delta = 0.14$. The open circles are experimental NMR data (Refs. 44–46).

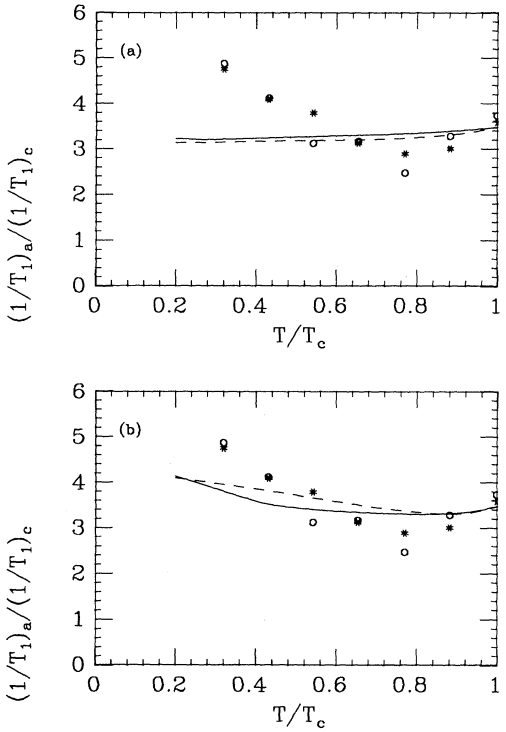

FIG. 12. (a) Shows the calculated temperature dependence of anisotropy ratio of Cu(2) for the s-wave state with $\psi_s = 2.5k_BT_c$ (dashed line) and $\psi_s = 1.76k_BT_c$ (solid line), respectively. The other parameters are the same as in Fig. 11. The points are the experimental data of Takigawa, Smith, and Hults (Ref. 44). The asterisks represent $(1/T_1)_c$ data taken by NQR and $(1/T_1)_a$ data taken by NMR in an external magnetic field of $H=0.44$ T. The open circle represent data taken by NMR in an external magnetic field of $H=0.44$ T. (b) Shows the calculated temperature dependence of anisotropy ratio of Cu(2) for d-wave (dashed line), and $s+id$ states (solid line). The parameters are the same as in Fig. 11.

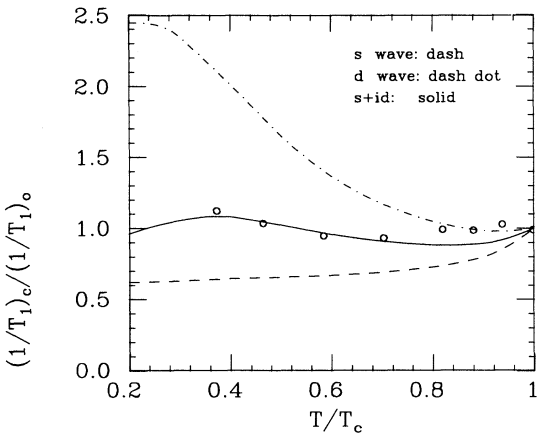

FIG. 13. Shows the calculated temperature dependence of the ratio of nuclear relaxation rate of Cu(2) ($\mathbf{H} \parallel c$ axis) and O(2,3) for s-wave (dashed line), d-wave (dotted line), and $s + id$ states (solid line). Here the ratio is normalized to its value at $T = T_c$. The parameters are the same as in Fig. 11. The points are the experimental NMR data (Refs. 45 and 46).

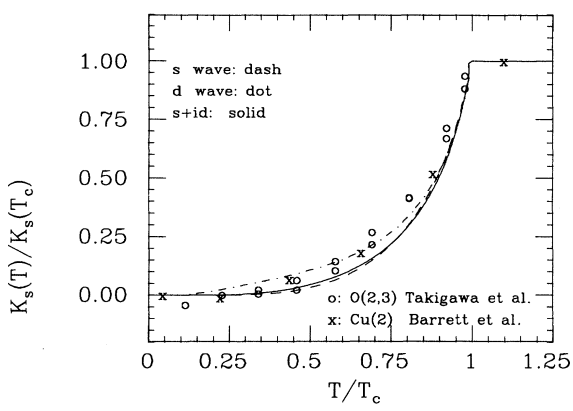

FIG. 14. Shows the calculated Knight shift as a function of temperature for s-wave (dashed line), d-wave (dotted line), and $s + id$ states (solid line). The parameters are the same as in Fig. 11. The points are experimental result of Takigawa *et al.* (Refs. 46 and 49) on O(2,3) and Barrett *et al.* (Ref. 50) on Cu(2).

the calculated temperature dependence of the ratio of $(1/T_1)_c$ of Cu(2) and $(1/T_1)_O$ of oxygen O(2,3) for various pairing states. We find that neither the s-wave nor d-wave state is in agreement with the experiment, and only the $s + id$ state can fit the experimental data. Again we emphasize that this conclusion is a qualitative feature of the calculation and is independent of the choice of $\psi_s(0)$ and $\psi_d(0)$.

Next we calculate the Knight shift which is proportional to the long-wavelength static susceptibility,[48]

$$\chi(q \to 0, \omega = 0) = -\sum_{\mathbf{p}} \frac{\partial n_F(E_p)}{\partial E_p}. \tag{30}$$

Again we fit the experimental data of Takigawa *et al.*[46,49] and Barrett *et al.*[50] using s-wave, d-wave, and $s + id$ states. A typical calculated Knight shift as a function of temperature is shown in Fig. 14 together with the experimental result. We find that the Knight shift can be fitted by either s-wave or $s + id$ states. It is very difficult to fit the Knight shift data with a pure d-wave state, especially in the low-temperature region where the Knight shift depends linearly on the temperature T for a d-wave state due to the nodes on the Fermi surface,[41] while the experimental data seem to be quite flat in the low-T region.

To summarize the NMR results, we find that although one can eliminate the Hebel-Slichter peak for an s-wave pairing state with a large scattering rate Γ, the s-wave state fails to explain the temperature dependence of the anisotropy ratio $(1/T_1)_a/(1/T_1)_c$ of Cu(2). Both d-wave and $s + id$ states, however, can explain the $(1/T_1)_a/(1/T_1)_c$ data qualitatively. The Knight-shift data, on the other hand, seem to suggest a nodeless gap function, which is inconsistent with d-wave pairing. If one looks at the overall experimental situation, only the $s + id$ state seems able to fit *both* the Knight-shift *and* $1/T_1$ measurements. Our conclusion is further supported by a special set of experimental data, namely, the ratio of relaxation rates of Cu(2) ($\mathbf{H} \parallel c$ axis) and O(2,3) nuclei, $(1/T_1)_c/(1/T_1)_O$, which can be fit by neither a s-wave nor d-wave state. Only the $s + id$ state can give a reasonable fit to the $(1/T_1)_c/(1/T_1)_O$ data.

We have also studied the effect of the shape of the Fermi surface (FS) on $1/T_1$. It has been suggested by Zha, Si, and Levin based on neutron-scattering experiments and band-structure calculations that the FS of $La_{2-x}Sr_xCuO_4$ is quite different from that of $YBa_2Cu_3O_7$.[51] The FS of $La_{2-x}Sr_xCuO_4$ is more like the FS of a simple tight-binding model on a 2D square lattice, while the FS of $YBa_2Cu_3O_7$ is rotated by 45° relative to the FS of $La_{2-x}Sr_xCuO_4$. The FS of $YBa_2Cu_3O_7$ mapped out by photoemission studies is in agreement with band-structure calculations and confirms the 45° rotated FS.[52] We have calculated $1/T_1$ for various pairing states using the single-particle dispersion of Eq. (22) with $t_2 = -0.5t$ which gives a 45°-rotated FS approximately. We find that the change of FS shape has a quite dramatic effect on $1/T_1$. In Fig. 15 we show the calculated temperature dependence of the anisotropy ratio of Cu(2), $(1/T_1)_a/(1/T_1)_c$, for various pairing states, including the B_1 d-wave state [Eq. (12)], the B_2 d-wave state [$\Delta(\mathbf{k}) = \psi_d \sin k_x \sin k_y$], and the mixed states of s waves (A_1) with B_1 and B_2 d waves. We can see that none of them is in agreement with the experiment qualitatively. Obviously a 45°-rotated Fermi surface with a B_2 d-wave state is *not* equivalent with the unrotated FS with a B_1 d-wave state because the hyperfine coupling $G(\mathbf{q})$ has fixed the coordinate system. We are currently working on the question of whether the $(1/T_1)_a/(1/T_1)_c$ data of $YBa_2Cu_3O_7$ can be understood with a more realistic FS, i.e., a 45°-rotated FS, in the framework of the one-band theory of Zhang and Rice[6] and the results will be published in a future publication.

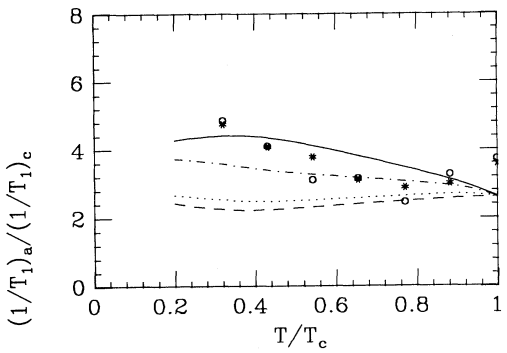

FIG. 15. Shows the calculated temperature dependence of anisotropy ratio of Cu(2) for the B_1 d-wave (solid line), the B_2 d-wave (dashed line), the $A_1 + iB_1$ (dot-dashed line), and the $A_1 + iB_2$ states (dotted line) using the 45°-rotated Fermi surface. Here A_1 is the s-wave state. The parameters used are $t = 20k_BT_c$, $t_2 = -0.5t$, $U = 2.25t$, and the hole doping $\delta = 0.2$.

VII. DISCUSSION

The purpose of this paper has been to examine the question of which superconductivity state is the ground state of the high-T_c materials. Early measurements of the penetration depth supported the s-wave picture, though measurements of this quantity at low temperatures ($T/T_c < 0.1$) had rather large errors.[29] Knight-shift measurements also appeared to support the s-wave picture, being nearly temperature independent at low temperature. Since most conventional theories gives rise to s-wave states, this situation seemed satisfactory from a theoretical point of view as well. At the same time, there were hints of gap anisotropy in Raman-scattering experiments, while difficult-to-evaluate tunneling and optical data appeared to show a softer gap than in conventional low-T_c materials.[19]

The nuclear relaxation rate data for the various nuclei in $YBa_2Cu_3O_7$ have changed this situation considerably. These data have very detailed temperature dependences which strongly constrain theory. Lu demonstrated that they are incompatible with s-wave theory and demand momentum-dependent coherence factors for their explanation.[40] Bulut and Scalapino analyzed a number of experiments to show that d-wave coherence could give a rather comprehensive explanation of these data.[41] In this paper, we have used a similar computational method to show that the $s + id$ state can improve the agreement of theory and experiment. This is particularly true of the Knight shift, whose temperature dependence is well described as activated in the low-temperature region. Similar success is found for the $s + id$ state in describing the temperature dependence of the penetration depth. The weak-coupling methods used in these calculations do not seem entirely appropriate to us; they are sufficient to establish, however, that momentum dependence of the coherence factors and probably also a hard gap are necessary to achieve qualitative agreement with experiment. The $s + id$ state has these features. In addition it has roughly the right amount of anisotropy under 45° in-plane rotations to explain angle-resolved photoemission experiments. These results are the best argument against pure d-wave pairing which currently exist. The d-wave state must definitely have nodes.

In the theoretical side, s-wave pairing is predicted by calculations starting from marginal Fermi-liquid theory as well as theories based on conventional ideas (phonons, etc.), while d-wave pairing follows from spin fluctuation theories using a phenomenological interaction. We have shown here that the $s+id$ (or possibly $s+d$) state follows from the t-J model, which probably describes the low-lying energetics well. Our method is variational. This means that we can never exclude the possibility that a better state exists. Extensive efforts along these lines have convinced us that obvious candidates do not work. The rough agreement of the calculated and observed condensation energies lends further support to this conclusion. Finite temperature calculations on the Hubbard model have tended not to show superconductivity. Our belief is that the rather complex momentum-space structure of unconventional superconductivity is difficult to achieve in small systems. We have presented numerical evidence to support this argument.

Note added in proof. Recently, a negative result for circular dichroism in $YBa_2Cu_3O_7$ has been obtained [T. W. Lawrence, A. Szoke, and R. B. Laughlin, Phys. Rev. Lett. **69**, 1439 (1992)]. This is consistent with $s + id$ singlet symmetry, since all singlet states give no signal in this experiment, in spite of the fact that the $s + id$ singlet state breaks the time reversal symmetry formally [Q. P. Li and R. Joynt, Phys. Rev. B **44**, 4720 (1991)]. Evidence from angle-resolved photoemission for gap anisotropy, consistent with d or $s + id$ symmetry, has been obtained by Z. X. Shen *et al.* [Phys. Rev. Lett. **70**, 1553 (1993)].

ACKNOWLEDGMENTS

We thank Dr. Jian Ping Lu, Dr. Dan Cox, Dr. Marshall Onellion, and Y. Zha for valuable conversations. This work was supported by the NSF through Grant No. DMR 9214739, and by the Electric Power Research Institute. We also acknowledge support from San Diego Supercomputer Center. B.E.C.K. was supported by the National Science Foundation.

[1] M. L. Cohen and P. W. Anderson, in *Superconductivity in d- and f-Band Metals (Rochester)*, Proceedings of the Conference on Superconductivity, in d- and f-Band Metals, edited by D. H. Douglas, AIP Conf. Proc. No. 4 (AIP, New York, 1972), p. 17, and reference therein.

[2] P. Morel and P. W. Anderson, Phys. Rev. **125**, 1263 (1962).

[3] A. J. Leggett, Rev. Mod. Phys. **47**, 331 (1975); Ann. Phys. (N.Y.) **85**, 11 (1974).

[4] D. Vollhart and P. Wolfle, *The Superfluid Phases of Helium 3* (Taylor & Francis, London, 1990).

[5] K. Miyake, S. Schmitt-Rink, and C. M. Varma, Phys. Rev. B **34**, 6554 (1986).

[6]F. C. Zhang and T. M. Rice, Phys. Rev. B **37**, 3759 (1988).
[7]E. B. Stechel, in *High Temperature Superconductivity*, edited by K. S. Bedell, D. Coffey, D. E. Meltzer, D. Pines, and J. R. Schrieffer (Addison-Wesley, Redwood City, 1990).
[8]M. S. Hybertsen, E. B. Stechel, M. Schlutter, and D. R. Jennison, Phys. Rev. B **41**, 11068 (1990).
[9]F. Mila and T. M. Rice, Physica C **157**, 561 (1989).
[10]A. J. Millis, H. Monien, and D. Pines, Phys. Rev. B **42**, 167 (1990).
[11]J. M. Wheatley, T. C. Hsu, and P. W. Anderson, Nature **333**, 121 (1988); Phys. Rev. B **37**, 5897 (1988); T. C. Hsu and P. W. Anderson, Physica C **162-64**, 1445 (1989); P. W. Anderson (unpublished).
[12]U. Welp, M. Grimsditch, S. Fleshler, W. Nessler, J. Downey, G. W. Crabtree, and J. Guimpel, Phys. Rev. Lett. **69**, 2130 (1992).
[13]C. Meingast, O. Kraut, T. Wolf, H. Wuhl, A. Erb, and G. Muller-Vogt, Phys. Rev. Lett. **67**, 1634 (1991); O. Kraut, C. Meingast, G. Brauchle, and H. Claus, A. Erb, G. Muller-Vogt, and H. Wuhl, Physica C **205**, 139 (1993).
[14]For a more detailed description of the VMC method, see, for example, C. Gros, R. Joynt, and T. M. Rice, Phys. Rev. B **36**, 381 (1987); C. Gros, Ann. Phys. (N.Y.) **189**, 53 (1989).
[15]D. J. Scalapino, in *High Temperature Superconductivity*, edited by K. S. Bedell, D. Coffey, D. E. Meltzer, D. Pines, and J. R. Schrieffer (Addison-Wesley, Redwood City, 1990), and reference therein.
[16]P. Monthoux, A. Balatsky, and D. Pines, Phys. Rev. Lett. **67**, 3448 (1991); P. Monthoux and D. Pines, *ibid.* **69**, 961 (1992); N. E. Bickers, D. J. Scalapino, and S. R. White, *ibid.* **62**, 961 (1989).
[17]A. J. Millis, Phys. Rev. B **45**, 13047 (1992); R. J. Radtke, S. Ullah, K. Levin, and M. R. Norman, *ibid.* **46**, 11975 (1992).
[18]J. F. Annett, N. Goldenfeld, and S. R. Renn, in *Physical Properties of High Temperature Superconductors II*, edited by D. M. Ginsberg (World Scientific, Singapore, 1990).
[19]B. Batlogg, in *High Temperature Superconductivity*, edited by K. S. Bedell, D. Coffey, D. E. Meltzer, D. Pines, and J. R. Schrieffer (Addison-Wesley, Redwood City, 1990).
[20]Q. P. Li and R. Joynt, Phys. Rev. B **47**, 530 (1993).
[21]G. J. Chen, R. Joynt, F. C. Zhang, and C. Gros, Phys. Rev. B **42**, 2662 (1990).
[22]R. Joynt, Phys. Rev. B **41**, 4271 (1990).
[23]See, for example, J. P. Elliott and P. G. Dawber, *Symmetry in Physics* (Oxford University Press, New York, 1984), Vol. 1.
[24]G. Kotliar, Phys. Rev. B **37**, 3664 (1988).
[25]C. Meingast (private communication).
[26]D. Ceperley, G. V. Chester, and M. H. Karlos, Phys. Rev. B **16**, 3081 (1977).
[27]D. J. Scalapino, S. R. White, and S. C. Zhang, Phys. Rev. Lett. **68**, 2830 (1992).
[28]W. E. Pickett, Rev. Mod. Phys. **61**, 433 (1989).
[29]D. R. Harshman, L. F. Schneemeyer, J. V. Waszczak, G. Aeppli, R. J. Cava, B. Batlogg, L. W. Rupp, E. J. Ansaldo, and D. Ll. Williams, Phys. Rev. B **39**, 851 (1989).
[30]A. T. Fiory, A. F. Hebard, P. M. Mankiewich, and R. E. Howard, Phys. Rev. Lett. **61**, 1419 (1988).
[31]J. Annett, N. Goldenfeld, and S. R. Renn, Phys. Rev. B **43**, 2778 (1991).
[32]J. M. Pond, K. R. Carroll, J. S. Horwitz, D. B. Chrisey, M. S. Osofsky, and V. C. Cestone, Appl. Phys. Lett. **59**, 3033 (1991).
[33]S. M. Anlage, B. W. Langley, G. Deutscher, J. Halbritter, and M. R. Beasley, Phys. Rev. B **44**, 9764 (1991).
[34]M. Prohammer and J. P. Carbotte, Phys. Rev. B **43**, 5370 (1991).
[35]M. Onellion (private communication); Y. Hwu, R. J. Kelley, G. Margaritondo, and M. Onellion (unpublished).
[36]For a recent review of NMR results on high-T_c superconductors, see, for example, C. H. Pennington and C. H. Slichter, in *Physical Properties of High Temperature Superconductors II*, edited by D. M. Ginsberg (World Scientific, Singapore, 1990); R. E. Walstedt and W. W. Warren, Jr., Science **248**, 1082 (1990).
[37]N. Bulut, D. W. Hone, D. J. Scalapino, and N. E. Bickers, Phys. Rev. Lett. **64**, 2723 (1990); Phys. Rev. B **41**, 1797 (1990).
[38]J. P. Lu, Q. Si, J. H. Kim, and K. Levin, Phys. Rev. Lett. **65**, 2466 (1990); B. S. Shastry, *ibid.* **63**, 1288 (1989).
[39]H. Monien and D. Pines, Phys. Rev. B **41**, 6297 (1990).
[40]J. P. Lu, Mod. Phys. Lett. B **6**, 547 (1992).
[41]N. Bulut, D. J. Scalapino, and R. T. Scalettar, Phys. Rev. B **45**, 5577 (1992); N. Bulut and D. J. Scalapino, Phys. Rev. Lett. **67**, 2898 (1991); **68**, 706 (1992); Phys. Rev. B **45**, 2371 (1992).
[42]V. Jaccarino, in *Theory of Magnetism in Transition Metals*, Proceedings of the International School of Physics "Enrico Fermi," Course XXXVII, Varenna, 1966, edited by W. Marshall (Academic, New York, 1967).
[43]See Ref. 41. We use the RPA susceptibility for ease of calculation and comparison to other results. Any enhancement function f, where $\chi = f(\chi_0)$, which is nonlinearly increasing will give results similar to those we present. Some such enhancement is dictated by normal-state experiments and to obtain the correct value of $(1/T_1)_a/(1/T_1)_c$ at $T = T_c$.
[44]M. Takigawa, J. L. Smith, and W. L. Hults, Physica C **185-189**, 1105 (1991); Phys. Rev. B **44**, 7764 (1991).
[45]P. C. Hammel, M. Takigawa, R. H. Heffner, Z. Fisk, and K. C. Ott, Phys. Rev. Lett. **63**, 1992 (1989).
[46]M. Takigawa, P. C. Hammel, R. H. Heffner, Z. Fisk, K. C. Ott, and J. D. Thompson, Physica (Amsterdam) C **162-164**, 853 (1989).
[47]L. Coffey, Phys. Rev. Lett. **64**, 1070 (1990).
[48]K. Yosida, Phys. Rev. **110**, 769 (1958).
[49]M. Takigawa, P. C. Hammel, R. H. Heffner, and Z. Fisk, Phys. Rev. B **39**, 7371 (1989).
[50]S. E. Barrett, D. J. Durand, C. P. Pennington, C. P. Slichter, T. A. Friedmann, J. P. Rice, and D. M. Ginsberg, Phys. Rev. B **41**, 6283 (1990).
[51]Y. Zha, Q. Si, and K. Levin, Physica C **201**, 289 (1992); Q. Si, Y. Zha, and K. Levin (unpublished).
[52]R. Liu *et al.*, Phys. Rev. B **46**, 11056 (1992).